**Atmospheric
Chemistry
and Physics
Discussions**

Analysis of accurate ^{13}C and ^{18}O isotope measurements of CO$_2$ in CARIBIC aircraft air samples from the tropical troposphere, and the upper troposphere/lowermost stratosphere

S. S. Assonov[1,2,*], C. A. M. Brenninkmeijer[2], T. J. Schuck[2], and P. Taylor[1]

[1]European Commission, Joint Research Centre, Institute for Reference Materials and Measurements, Geel, Belgium
[2]Max Planck Institute for Chemistry, Atmospheric Chemistry Division, Mainz, Germany
[*]presently at: Institute for Geology and Mineralogy, University of Köln, Germany

Correspondence to: S. S. Assonov (assonov_sergey@yahoo.com)

ACPD

10, 5999–6057, 2010

Analyses of CO$_2$ isotope data for tropical troposphere and UT/LMS

S. S. Assonov et al.

Title Page

Abstract	Introduction
Conclusions	References
Tables	Figures

	◄	►	
◄	►
Back	Close

Full Screen / Esc

Printer-friendly Version

Interactive Discussion

Abstract

The project CARIBIC (http://caribic-atmospheric.com) aims to study atmospheric chemistry and transport by regularly measuring many compounds in the free troposphere (FT) and the upper troposphere/lowermost stratosphere (UT/LMS) by using passenger aircraft. Here CO_2 concentrations and highly accurate isotope results are presented in detail together with supporting trace gas data. 509 CARIBIC-2 samples (highest precision and accuracy $\delta^{13}C(CO_2)$ and $\delta^{18}O(CO_2)$ data) from June 2007 until March 2009, together with CARIBIC-1 samples (flights between November 1999 and April 2002, 350 samples in total, 270 for NH, mostly $\delta^{13}C(CO_2)$ data) give a fairly extensive, unique data set for the NH free troposphere and the UT/LMS region. To compare data from different years a de-trending is applied. In the UT/LMS region $\delta^{13}C(CO_2)$, $\delta^{18}O(CO_2)$ and CO_2 are found to correlate well with stratospheric tracers, in particular N_2O. These correlations are in good agreement with current understanding of stratospheric circulation. $\delta^{18}O(CO_2)$ appears to be a useful, hitherto unused, tracer of atmospheric transport in the UT/LMS region. By filtering out the LMS data (based on N_2O distribution), the isotope variations for the free and upper troposphere are obtained. These show however little latitudinal gradient, if any, and are in good agreement with the data of selected NOAA stations in NH tropics. Correlations between $\delta^{13}C(CO_2)$ and CO_2 are observed both within single flight(s) covering long distances and for certain seasons. The overall variability in de-trended $\delta^{13}C(CO_2)$ and CO_2 for CARIBIC-1 and CARIBIC-2 are similar and basically agree with each other, which also underscores the high quality of measurement. Based on all correlations, we discuss that CO_2 distribution in the NH FT and UT (at CARIBIC flight routes) is regulated by uplift and pole-wards transport of tropical air up to approximately 50° N. The main reasons for variability of signals in FT and UT (which is larger for the high spatial resolution sampling during CARIBIC-2) is mixing of different tropospheric air masses affected by CO_2 sources and sinks. The effect of stratospheric flux appears to be limited. All in all it is demonstrated that CARIBIC produced new important and reliable data sets for little

explored regions of the atmosphere. A logical next step will be global scale modeling of ^{13}C and especially ^{18}O, which is linked to the hydrological cycle.

1   Introduction

The global cycle of CO_2 is of extraordinary complexity and importance. The atmo-
5   spheric CO_2 reservoir is coupled to those of the oceans, soils, and vegetation and is increasingly burdened by emissions from the combustion of fossil fuel, while at the same time global temperatures increase concomitant with profound changes in vege-
tation, soils and oceans. Since the extensive paper by Callendar (1938) that already dealt with several aspects of the CO_2 cycle including climate effects, many more pub-
10   lications treat nearly all aspects of understanding all the complexities of the CO_2 cycle in even greater detail.

Large numbers of observations of CO_2 concentrations at land based stations and by using ship, aircraft and satellites are made with the goal to tackle the problem of sufficiently thoroughly understanding and quantifying the large fluxes between the at-
15   mosphere and the other reservoirs. The need for large numbers of measurements of atmospheric CO_2 is exemplified by for instance the Carbon America Program (http://www.nacarbon.org/nacp/) that involves numerous projects with a vast increase in the number of in situ measurements also by using towers and aircraft to take verti-
cal profiles. Besides concentration measurements, flux measurements are carried out,
20   other trace gases are used as proxies of fossil fuel derived CO_2 (Levin et al., 2008), the O_2/N_2 ratio is measured (Bender et al., 2005), and isotope measurements are con-
ducted. These comprise $^{14}CO_2$ measurements (Levin and Karstens, 2007; Turnbull et al., 2006) and stable isotope measurements.

Source and sink processes are accompanied by stable isotope fractionation which
25   induces isotope variations in atmospheric CO_2. Isotope measurement thus may give information about source and sink processes. The first measurements of atmospheric CO_2 and $^{13}C(CO_2)$ date from before 1960 (Keeling, 1961). The dominant signals con-

Full Screen / Esc

Printer-friendly Version

Interactive Discussion

tained in the major isotope ratios (i.e. disregarding ^{17}O and clumped isotope signals) are that the ^{13}C/^{12}C ratio is dominated by photosynthesis, respiration and burning whereas the ^{18}O/^{16}O ratio is strongly affected by isotope exchange with water, predominantly leaf and soil water. For instance, the large carbon sink of the terrestrial biosphere in the Northern Hemisphere (NH) was confirmed by analyses of gradients in ^{13}C(CO$_2$) (Ciais et al., 1995). For ^{13}C(CO$_2$) even an "Isolandscape" is available (Bowen et al., 2009) constructed by smoothening and interpolation many such data (Dlugokencky et al., 1994; Masarie and Tans, 1995). A recent paper by Rayner et al. (2008) reports on inverse modeling using ^{13}C(CO$_2$) and CO$_2$ mixing ratios, and communicates that model improvements and large ^{13}C data sets hold promise here. However, ^{18}O data have not been generated and used to the same degree by far, and contain different, perhaps more convoluted information that, however, ought to be fully understood and may hold useful applications (Still et al, 2009).

When endeavoring to estimate CO$_2$ fluxes and transport mixing with confidence, the number of atmospheric observations available worldwide appears still to be limited for crucial regions. Based on data of CO$_2$ observational networks Patra and co-authors (Patra and Maksyutov, 2002; Patra et al., 2003) concluded on the need to extend the network by optimally located stations in continental South America, Africa and Asia. One of the contributions to help to close the gap is to use aircraft observation platforms (13th_WMO/IAEA_Meeting, Expert Group Recommendations). In fact, Bischof and Bolin already in 1966 reported (Bischof and Bolin, 1966) on aircraft based CO$_2$ measurements.

CARIBIC (Civil Aircraft for the Regular Investigation of the atmosphere Based on an Instrument Container, www.caribic-atmospheric.com) uses a specially modified passenger aircraft that on a monthly basis conducts long distance measurement flights using an automated laboratory for real time measurements of trace gases and aerosol and even their sampling. Although CARIBIC basically is an atmospheric chemistry project, CO$_2$ measurements are part of its large measurement package. CO$_2$ is used as a tracer that helps to identify air masses, but in view of its great importance these

measurements have their own weight to help to tackle the "CO_2 problem".

CO$_2$ measurements in CARIBIC were and still are to a large degree based on the analysis of air samples, although an in situ analyzer for CO_2 is tested in CARIBIC 2. Having air samples available, it is a logical step to conduct stable isotope measure-
ments. Why? First, the overall project represents a significant technological, logistical and scientific effort. As such, the optimization of the scientific payload and its use is essential. Second, to our knowledge there are no other large scale, high accuracy systematic CO_2 isotope measurements in the free troposphere and UT/LS. Conversely, it is also evident that air samples collected at large distances from sources and sinks
mostly in background air require high quality analyses.

Therefore we measured, and here present and discuss in detail the results of accurate and precise CARIBIC CO_2 isotope analyses of a wide range of representative air masses in chiefly the Northern Hemisphere. To generalize this information and to organize the CARIBIC data set, a method is sought that groups the data according to
air mass chemical composition and origin (meteorological regime). Because the use of isotopic information is rather sporadic and the type of platform not used on a large scale either, our account is more extensive than fore more common topics. In the following we first give basic information about the CARIBIC platform, followed by details about the mixing and isotope ratio measurements and their quality. Second, we show
how the time series spanning 1997–2008 can be de-trended after which we explain which air masses are sampled and, third, apply tracer-tracer correlations to demonstrate the effect of UT/LMS mixing by optimal usage of chemical stratospheric tracers. Fourth, we discuss the data of the free tropical troposphere and UT region followed by a comparison of the CARIBIC time series with the extensive data from NOAA-ESRL.

Finally, we briefly discuss the future data use in models and address aspects of sampling and model resolution as well as the quality of analytical data. CARIBIC-1 and CARIBIC-2 give a good example of different resolution approaches. High resolution sampling helps to study in details various atmospheric effects involved, while lower resolution may be more compatible with the resolution of models. Though the

present data set is self-consistent, comparing and merging data produced in different laboratories is still a very critical issue.

2 Experimental

2.1 The CARIBIC observatory

CARIBIC (http://caribic-atmospheric.com) investigates atmospheric chemistry, transport and composition by measuring many compounds (long and shorter lived trace gases and aerosol) from regions on the globe reached from Europe using an automated laboratory aboard a passenger aircraft. The monthly repeated flights (presently 4 sequential long distance flights) over periods of years, covering large regions while measuring many species simultaneously provide data sets that are not otherwise available.

The flight tracks, dates and sampling locations are shown in Fig. 1. Nearly all information obtained is for cruise altitudes, i.e. between 9 and 12 km. (The lowest sampling altitude was ~7 km.) From such altitudes little regular detailed isotope information is available. Each long distance flight covers a wide range of meteorological conditions, opposite to land-based stations. Cruising in the mid-latitude upper troposphere/lowermost stratosphere and the tropical troposphere means that sampling is remote from CO_2 sources and sinks. However, convection and the larger scale uplift of air masses in weather systems can at times deliver air with a certain surface air affected component at cruising altitude. To give a number, ~35% of samples analyzed for 2007–2008 were from the UT-LMS at extra-tropical mid-latitudes. An inventory of air masses probed by CARIBIC-2, based on cluster analyses is given by Köppe et al. (2009). Schuck et al. (2009) present all CO_2 and other greenhouse gas data, whereas an overview for CARIBIC-1 is given by Zahn et al. (2002).

CARIBIC-1 operated from late 1997 until April 2002, using a Boeing 767 sampling on routes to and from the Maldives, Sri Lanka, Southern Africa, and the Caribbean.

Analyses of CO_2 isotope data for tropical troposphere and UT/LMS

S. S. Assonov et al.

Here each month 12 large air samples of nominally $\sim$340 L STP were taken during one flight leg (Brenninkmeijer et al., 1999). Each air sample represented a flight distance of $\sim$250 km. An initial overview of CARIBIC-1 isotope data was given at 14th CO_2 experts meeting in Helsinki, 2007 (Assonov et al., 2007), whereas details of isotope measurements and calibration are published in Assonov et al. (2009b).

CARIBIC-2 started its operation early 2005 based on an Airbus A340-600 from Lufthansa Airlines equipped with a sophisticated air inlet system carrying a totally new container (1.5 ton) with a multitude of analyzers (Brenninkmeijer et al., 2007). Here 28 samples are taken during 2 of the 4 monthly flight legs using glass flasks. In this case of normal sample size, resolution is higher with each sample representing only $\sim$15 km distance. Details of the sampling system and procedure are given by Schuck et al. (2009). Like in CARIBIC-1 both sampling and all (online) measurements during the flights are fully automated with air sampling being done at fixed time intervals fairly evenly spread along the flight track.

The sampling system, the number of samples, and the mass spectrometry for CARIBIC-2 are superior to that of CARIBIC-1, although even these data prove to be of high quality. Details of isotope measurements and calibration are published in Assonov et al. (2009a). CARIBIC-2, for April 2007 – March 2009 (which is the subset used for CO_2 isotope analyses), represents the latitudes 14 to 55° N covered by some flights to North America, but mostly the Philippines and India.

2.2 Concentration and isotope measurements

The CO_2 mixing ratios were obtained using gas chromatography with simultaneous measurement of CH_4, N_2O and SF_6. The analytical procedure and performance for CARIBIC-2 are given in detail by Schuck et al. (2009). The precision and total combined uncertainty for CO_2 are about 0.15 and 0.20 ppm respectively. For CARIBIC-1 no account has been published. Based on the assessment of many years performance of the analytical instruments, we assign precision and total combined uncertainty of 0.20 and 0.25 ppm to the CARIBIC-1 CO2 concentration measurements. CO_2 concentration

measurements are traced back to the WMO X2007 scale for CO_2-in-air by using NOAA ESRL standards.

All isotope data are on the VPDB-CO_2 scale (linked to NBS-19-CO_2) by using the ^{17}O correction after Assonov and Brenninkmeijer (2003) which is currently being officially recommended (13th_WMO/IAEA_Meeting; Brand et al., 2009). The NOAA-ESRL data produced using the ^{17}O correction by Alison et al. (1995), are corrected by us for the differences between the algorithms [Assonov – Allison] which can be approximated by

$$\Delta^{13}C(CO_2) = -[0.0031 \cdot \delta^{18}O(CO_2) + 0.030].$$

The CO_2 isotope analyses for CARIBIC-1 and CARIBIC-2 differ in many aspects, namely the aircraft sampling system, sample size, mass spectrometry and correction procedures; details are given by Assonov et al. (2009a, 2009b). CARIBIC-1 samples were analyzed at MPI-C, Mainz; CARIBIC-2 samples at JRC-IRMM, Belgium. In both cases proper calibration was confirmed by excellent agreement with NIST RMs CO_2 and Narcis-CO_2. For CARIBIC-2, an inter-comparison with MPI-BGC demonstrated a small, consistent scale discrepancy in $\delta^{13}C(CO_2)$ of -0.04‰ (data obtained at IRMM and MPI-BGC use the Assonov' ^{17}O correction algorithm) and $\delta^{18}O(CO_2)$ of -0.06‰ (details are given by Assonov et al., 2009a). This is much less than the variability discussed in the present paper, and less than inter-laboratory scale discrepancies recently published (e.g. Levin et al., 2007). 28 samples from a flight in March 2009 we also analyzed at MPI-BGC by using the same method as we used at JRC-IRMM; the data obtained at MPI-BGC are corrected for the inter-laboratory scale discrepancy observed.

Typical total uncertainties of the CARIBIC-1 and CARIBIC-2 CO_2 data are given in Table 1. Though the uncertainty for our isotope data (propagated to the primary scale) exceeds the inter-laboratory comparability targets set at 0.01‰ for $\delta^{13}C(CO_2)$ and 0.05‰ for $\delta^{18}O(CO_2)$ (13th_WMO/IAEA_Meeting, Expert Group Recommendations), the values appear to be to one of the best achieved values to date.

Isotope exchange between CO_2 and traces of H_2O is a known problem that leads

to artifacts of more negative $\delta^{18}O(CO_2)$ values. In CARIBIC-1 where stainless steel canisters of 20 liter at ~17 bar were used the data showed the problem of exchange. This improved in time, but persisted for some cylinders. The CARIBIC-1 data used are filtered according to negative $\delta^{18}O(CO_2)$ deviations (Assonov et al., 2009b). As the
5 remaining $\delta^{18}O(CO_2)$ results still might have been affected to a small but undefined degree, the CARIBIC-1 $\delta^{18}O(CO_2)$ are used qualitatively only.

In CARIBIC-2 2.7 liter glass flasks at ~4 bar are used and no effects of ^{18}O exchange between CO_2 and H_2O were detected. Only two samples were suspect and their data rejected. Independent proof of absence of isotope exchange in glass flasks
10 under aircraft conditions would require tests for which the means were not available. The frequency distribution of the values obtained, and the literature on the use of glass flasks given the fact that air at cruise altitude is very dry, render credibility to the assumption that no exchange in excess of measurement error has occurred. Moreover, several longer term storage tests showed only small $\delta^{18}O(CO_2)$ shifts.

15 **3   Observational data**

3.1   Overview of meteorology and trace gas measurements: Aspects specific for civil aircraft sampling with an overview of GHG data

CARIBIC data are gathered at different latitudes and longitudes within a narrow range of altitudes. One single flight covers a wide range of meteorological regimes such as
20 mid-tropospheric air in the tropics or upper tropospheric air and lower stratospheric air in mid- and high-latitudes. The flight tracks are depicted in Fig. 1. The cruise altitude during a single flight usually increases with fuel burnt, and typically ranges from 9 to 12 km. The mean/typical pressure altitude for CARIBIC 1 (Boeing 767) was 266±25 hPa (Median and 1StDev). For CARIBIC -2 (Airbus A340-600) this was
25 237±33 hPa for the period considered. Most CARIBIC instruments operate only at pressure altitudes of 500 hPa or less (higher altitude) to avoid contamination of the

sensitive analytical systems and thus little vertical profile information is available on this basis.

At mid-latitudes, flights always cross the tropopause and lowermost stratospheric air is frequently sampled. In such instances older air is probed implying that CO_2 mixing ratios are shifted backwards in time. At lower latitudes where the tropopause is higher, free sub-tropical and tropical air is encountered. We note that the return flights start initially at lower altitudes and reach over Europe deeper into the LMS. During the return flights meteorological conditions are usually similar to those of the outward bound flights, so that GHG and other profiles of forward and return flights nearly mimic each other. Relevant meteorological parameters (5 day back trajectories, potential vorticity cross sections along the flights etc.) for all CARIBIC flights are available at the KMNI web-site (http://www.knmi.nl/samenw/campaign_support/CARIBIC/). An example of meteorological parameters, and chemical tracers by CARIBIC-1 is given in Zahn et al. (2002).

Many other trace gases are measured on the air samples, but here we discuss, next to CO_2, $\delta^{13}C(CO_2)$ and $\delta^{18}O(CO_2)$), where applicable, only other main greenhouse gases namely CH_4, N_2O and SF_6. The 2 upper panels in Fig. 2 give the 4 scatter plots for CARIBIC-2 against O_3 for which the latter data from continuous recording were integrated aver the sampling intervals. For the other greenhouse gases namely CO_2, CH_4, N_2O and SF_6 one can discern mixing trends towards LMS air (high O_3) with a large variability for UT and FT air masses (O_3 values typically below 100 ppb). For N_2O tropospheric variability is lowest. For SF_6 the relative uncertainty is lowest, but the scatter for tropospheric samples is mostly due to the effect of its localized sources. CH_4 for that reason also shows tropospheric scatter, but otherwise shows a compact mixing line. CO_2 concentrations demonstrate the largest variability for UT and FT air masses mainly due to its seasonal cycle and its increasing trend. The variability propagates into the lowermost stratosphere while being continuously attenuated by ongoing mixing with LMS air.

Below we aim to demonstrate how CO_2 isotope data reflect the two dimensions of

variability, namely in UT and FT air masses and in the mixing trend towards LMS air. We also show in Fig. 2 by using sampling interval integrated continuous CO values, the O$_3$ excess versus the chemical tropopause as defined by Zahn et al. (2004b) and N$_2$O versus CO. For discriminating tropospheric and stratospheric samples one can use in principle physical tracers (e.g. PV values) or one of the chemical tracers N$_2$O, SF$_6$, CH$_4$ and O$_3$ (lower panels in Fig. 2). Later in the manuscript we will select the most suitable tracer for this purpose, namely N$_2$O.

3.2 Data de-trending

For comparing the CARIBIC-1 and CARIBIC-2 CO$_2$ data which together cover 10 years, with a break of about 5 years, a de-trending is necessary in view of the trends in CO$_2$, δ^{13}C(CO$_2$) and N$_2$O. We base the de-trending factors (Table 2) on the NOAA flask data obtained for remote stations in the NH tropics. First, monthly means were used to obtain annual averages, upon which for CO$_2$ and N$_2$O the average slopes of the linear fits are established. In this way all CARIBIC data are de-trended to 01/01/2007.

The de-trending procedure introduces errors which are manifest as deviations from the fit lines (Fig. 3). However, the linear fit for CO$_2$ captures nearly all of the variance over the years of the interest with deviations between -1 to 0.5 ppm. Therefore higher order fits (Masarie and Tans, 1995) are not applied.

If trends in CO$_2$ and δ^{13}C(CO$_2$) are caused by common processes, the δ^{13}C(CO$_2$) decrease must be consistent with the inferred CO$_2$ increase. Combination of the δ^{13}C(CO$_2$) trend (Fig. 3) and the CO$_2$ increase rate (Table 2) results in an annual δ^{13}C(CO$_2$) decrease rate. The trends for these remote stations agree well (for MLO and KUM the intercepts of -14.2 and -14.0‰; the trend for MID shows the same slope but some offset). Plotting δ^{13}C(CO$_2$) vs. year (not shown) gives basically the same slope but this cannot demonstrate a consistency between δ^{13}C(CO$_2$) and CO$_2$ increase rates.

Errors for the δ^{13}C(CO$_2$) de-trending are not easily quantified. First, the annual

δ^{13}C(CO$_2$) decrease is nearly of the same magnitude as the long term analytical accuracy. Second, also variability of seasonal circulation patterns (e.g. discussed for CO$_2$ at Mauna Loa by Lintner et al., 2006) causes variability in air mass composition and CO$_2$ signals at stations. The first estimate of errors may be given by δ^{13}C(CO$_2$) deviations relative to the linear fit which are mostly within 0.025‰, with one value deviating by about 0.05‰ (Fig. 3).

The linear fit for N$_2$O (Fig. 3) captures the change over the years of interest, with 2001 and 2002 showing higher increases, and 1999 a lesser increase. The mean slope of 0.76 ppb/y (Table 2, years 1998 to 2008) appears to agree with values obtained over 1994 to 2006 for several NOAA stations (a range from 0.76 to 0.85), with the global cosine-weighted average of 0.80 (Jiang et al., 2007). Deviations from the linear fit to the NOAA data do not exceed 0.5 ppb (Fig. 3). De-trended monthly means for the stations MLO, KUM, IZO, AZR show nearly identical distributions, with medians of 320.7 ppb and 1 St. Dev. of 0.3 ppb (Fig. 4, upper panel). The distributions are slightly skewed, possibly due to the anomalous increase of N$_2$O in 2000 and 2001 (Fig. 3, see also Jiang et al., 2007). Here, variability in air mass composition (e.g. Mauna Loa, Lintner et al., 2006) may also play a role. The distribution widths include both seasonal variations and errors introduced by data de-trending. The fact that several stations in the NH tropics have narrow and nearly identical distributions of N$_2$O, with maximal deviations from the median within 0.9 ppb (3-σ), implies that the N$_2$O distribution can be used to construct the filter applied to separate FT and UT air from the LMS air discussed in the following.

3.3 Use of tracers to distinguish LMS air masses from FT plus UT air masses

In order to analyse the results, the CARIBIC-1 and CARIBIC-2 data are separated in two pools representing (i) tropospheric air, i.e. FT plus UT air masses, and (ii) LMS air and air masses resulting from UT/LMS mixing processes. Because CARIBIC covers different latitudes, altitudes and seasons, and high resolution samples are taken,

Full Screen / Esc

Printer-friendly Version

Interactive Discussion

choosing an appropriate separation criterion is not trivial. Particularly the fact that CO_2 is a long lived tracer means that each sample typically contains a mixture of air masses of different history. Back-trajectories of 5 or 8 days as commonly used in CARIBIC chemical studies are not sufficiently informative, whereas prolonged back-tracking of air masses makes little sense in view of uncertainties in transport and mix-ing. Using modeled potential vorticity (PV) values demonstrates a large scatter (not plotted), with occasionally values of up to 5 PV for air masses which are considered to be tropospheric based on O_3 being below the chemical tropopause and high N_2O. (Tropospheric air masses are typically considered to have PV from 0 to 2.5, whereas stratospheric air masses have higher values).

A common criterion for separating air masses is based on the aforementioned chem-ical tropopause. Whereas pure meteorological tropopause definitions (like PV) may not have the required resolution, the chemical tropopause is an operational concept based on gradients of contrasting tracers measured in situ. Using the stratospheric tracer O_3 and the contrasting tropospheric tracer CO (typically giving the characteristic L-shape mixing plots, cf. Fig. 2), Zahn et al. (2004b) introduced an ozone based chem-ical tropopause with a seasonally varying boundary level of O_3. Different groups (Pan et al., 2004; Hoor et al., 2004, 2005) also demonstrated that use of chemical tracers and the chemical tropopause is truly informative to describe mixing of air masses of different origin in the UT/LMS region. The applicability of chemical tracers was even proven in case of double thermal tropopause occurrences in the extra-tropics (Pan et al., 2007).

For discrete UT/LMS events of CARIBIC-1 it was shown that $\delta^{13}C(CO_2)$ correlated well with the O_3 excess vs. the chemical tropopause (Assonov et al., 2007). However, due to a limited data set, low sampling resolution and problems with flasks, the same was not shown for different seasons and $\delta^{18}O(CO_2)$. In particular, O_3 variability and seasonality in LMS may play a role. When aiming to construct a robust filter to sepa-rate LMS air masses for the whole data set, the use of O_3 needs to be compared with another suitable candidate, namely N_2O. An obvious reason to consider N_2O is that its

lifetime better matches that of CO_2 than that of O_3. At the outset there are some disadvantages associated with the use of O_3. i) Stratospheric O_3 has a seasonal variability due to production changes (e.g. Hegglin and Shepherd, 2007) whereas the long lifetime of N_2O results in a gradual destruction. Indeed, N_2O plotted vs. O_3 for CARIBIC-2 (Fig. 2, upper panel) shows a clear variability of slopes at higher values; ii) Photochemical production and destruction of O_3 in the troposphere (Zahn et al., 2002) leads to variability as well. This is visible in Fig. 2 (lower panel, O_3 vs. CO and histogram) – the peak at O_3 below the ozone tropopause level is not compact. Some samples having low O_3 (accordingly classified as UT air) have also low N_2O (not plotted) and must actually be considered to be LMS air. Conversely, some samples with O_3 in excess of the chemical tropopause level, also have high N_2O, and thus are definitely tropospheric.

In contrast to O_3, N_2O demonstrates a compact and narrow peak at high N_2O (Fig. 2, lower panel) with tailing towards lower values corresponding to the LMS contribution. This as well as the compact distribution of N_2O for stations (Fig. 4) implies that a certain N_2O level may be used as a cut-off providing a robust filter for LMS and LMS-affected air masses. There are compelling reasons to use N_2O. i) N_2O has been successfully used to describe the UT/LMS mixing (Hoor et al., 2004), we cite: "...tropospheric N_2O is well mixed giving a rather constant tropospheric mean value... It's major sink is in the tropical stratosphere where it is destroyed via photolysis and reaction with $O(^1D)$. The long local photochemical lifetime ... leads to much weaker N_2O-gradients at the tropopause than for O_3, but makes it ideal to trace stratospheric transport since N_2O is not affected by local photochemistry. ...."; ii) CO_2 oxygen isotope changes in the stratosphere correlate better with N_2O than with O_3 (Boering et al., 2004). These authors consider N_2O as tracer giving an effective reaction time for CO_2 oxygen isotope changes; iii) N_2O data are obtained on the same air samples as used for CO_2 isotope analysis which excludes any uncertainty related to integration of continuous ozone data over the sampling interval.

Despite N_2O offering advantages, its application has been limited for chiefly two reasons: (i) High precision N_2O measurements, being lab based using flask samples,

Analyses of CO_2 isotope data for tropical troposphere and UT/LMS

S. S. Assonov et al.

are rare, whereas O_3 data are obtained routinely at high resolution; (ii) the ratio of O_3 variability to precision is about 500 (range 500 ppb, precision 1 ppb), whereas the ratio for N_2O is only about 80 (range 25 ppb, precision 0.3 ppb).

When using N_2O one has to decide on the appropriate cut-off level. The distribution for CARIBIC-2 (de-trended to 01/01/2007) has a distinct peak with the median at 321.3 ppb (Fig. 4, lower panel), CARIBIC-1 data show the same features. Although a cut-off of 320.0 ppb is selected arbitrarily, this is a safe approach - the distance [the peak median minus the cut-off level] being 1.3 ppb slightly exceeds both the half-width of the CARIBIC peak (Fig. 4, lower panel) and also the maximal seasonal variability of N_2O in the NH tropics (3-σ of 0.9 ppb, Fig. 4, upper panel).

Finally we note that we had to use for CARIBIC-1 a slightly higher N_2O increase rate, actually 0.90 ppb/y instead of 0.76 ppb/y, to have the median in agreement with CARIBIC-2. Furthermore, the N_2O peak median (FT and UT air) for CARIBIC-2 de-trended data (Fig. 4, lower panel) is higher than the medians (∼320.7 ppb) obtained for background NOAA stations in the NH tropics. This disagreement as well as the higher de-trending factor needed for CARIBIC-1 most likely relates to a small N_2O scale inconsistency between NOAA and MPI-C Mainz. Addressing this problem is beyond the scope of our paper. (We note that the summer monsoon samples from June-September 2008 might have shifted the distribution to higher N_2O, by 0.2 to 0.3 ppb.)

4 Discussion

4.1 CO_2 isotope data for LMS air masses

4.1.1 Examples of flights that sampled LMS air masses

CARIBIC-2 flights (high resolution sampling) crossing LMS air masses have recorded detailed correlations for a range of trace gases (Fig. 5). Such events are well recorded by concomitant CO and O_3 values reflecting UT/LMS mixing (L-shape mixing plots), but

also by lower N$_2$O, CH$_4$ and SF$_6$ values. At times detailed and clear L-shape mixing plots (similar to the L-shaped plot of O$_3$ vs. CO plots) are obtained for CO$_2$, δ^{13}C(CO$_2$) and for δ^{18}O(CO$_2$), (the right column in Fig. 5, data given vs. N$_2$O reversed scale) implying that UT/LMS mixing can be reflected by CO$_2$ isotopes. Such correlations due

5 to UT/LMS mixing have been observed for 14 out of 21 flights.

As pointed out, outward bound and corresponding return flights usually cross nearly the same stratospheric structures (folds, intrusions and filaments), resulting in nearly symmetrical PV and GHG profiles. In such cases the UT/LMS mixing lines for CO$_2$, δ^{13}C(CO$_2$) and for δ^{18}O(CO$_2$) (or some of the signals) start from the same strato-

10 spheric end-member. A large variability in the composition of UT plus FT air masses over a single flight is often observed, implying a variety of air masses taking part in the LMS ventilation and/or the UT air masses mixed-in/transported directly to this region (being close to the stratospheric folds, intrusions and filaments).

By binning CARIBIC-2 flights that probed the UT/LMS in 4 seasons (Fig. 6, only

15 latitudes above 35° N are plotted), one can observe a similarity of the stratosphere-enriched end-member's composition, with somewhat variable degree of this enrichment (lowest N$_2$O in different seasons is different), while the variability of the slopes of the mixing trend lines (the L-shape plots) is large. The latter strongly depends on the variability of UT component(s), while also a variable regime of LMS ventilation (e.g.

20 Zahn et al., 2004a) plays a role. We also note that different stratospheric enrichment recorded in different seasons might also be due to variable thickness of the LMS mixing reservoir and variable altitude of the tropopause. (Flight corridors cover a limited range of altitudes.) The CO$_2$ and δ^{13}C(CO$_2$) plots appear to be nearly perfect mirror images, which is expected because δ^{13}C(CO$_2$) vs. 1/CO$_2$ in the troposphere share source and

25 sink processes.

4.1.2   General picture of UT/LMS mixing

As CARIBIC-2 flight routes cover different regions (Fig. 1), we can conclude that CARIBIC has recorded rather general features of UT/LMS mixing in large parts of the NH. To demonstrate a more general picture of CO$_2$ isotope distribution in the UT/LMS
5 region and similarity of the stratospheric component over different seasons (note, data coverage for some seasons is limited), we plot the data of all CARIBIC 1 + 2 flights crossing the UT/LMS (Fig. 7). On this plot we separate data for latitudes >35° N affected by UT/LMS mixing and latitudes <35° N which are not affected directly.

Triangle-shaped mixing areas are observed for CO$_2$, δ^{13}C(CO$_2$) and δ^{18}O(CO$_2$),
10 with CARIBIC-1 and CARIBIC-2 showing the same features. The triangles are formed by seasonally variable signals of UT air masses (Fig. 6). The largest variability of CO$_2$ and isotope signals is within a narrow range of (high) N$_2$O values (Figs. 6, 7) which corresponds to FT and UT air masses. This is both due to seasonal variations and different degrees of mixing of air masses affected by sources and sinks and background
15 air masses as discussed below. The variability in CO$_2$ and δ^{13}C(CO$_2$) demonstrated by CARIBIC-2 (high-resolution sampling) is larger than that of CARIBIC-1 whereas the general relationships are very similar, except for δ^{18}O(CO$_2$) (negative shifts due to exchange in canisters). This agreement exists despite different flight routes (Fig. 1) and different years of observation.

20 Towards the stratospheric end member (low N$_2$O), the variability in all signals diminishes, apparently indicating a single end member mixing ratio (Fig. 7). (All data are de-trended to 01/01/2007). This reflects CO$_2$ signatures of ascending tropical air (examples are KUM, MLO and MID, Fig. 9, see below) that enters the stratosphere and returns at NH mid-latitudes with some δ^{18}O(CO$_2$) modifications. In fact, the back-
25 flux of stratospheric air into the UT does not constitute a single component because it consists of a mixture of air masses having had different stratospheric residence times (age distribution) (Hall et al., 1999; Andrews et al., 2001; Engel et al., 2009) with a tailing towards older stratospheric air. The stratospheric circulation also attenuates the

CO_2 seasonal cycle of ascending air by mixing during transport (Andrews et al., 2001; Strahan et al., 1998). The mean of the age distribution can be approximated by an apparent age, which is defined by decreases of tracers (such as N_2O, CO_2 and SF_6) vs. the signals measured in tropospheric air. The highest apparent SF_6 age for strato-
5   spheric samples of CARIBIC-1 is up to 2 years (not plotted). Given that the lowest N_2O values for CARIBIC-1 are about the same as for CARIBIC-2 (Fig. 7), the apparent ages are to be the same.

The stratospheric flux at mid latitudes is first transported to an intermediate reservoir, namely the LMS as recognized by using CO and O_3 correlations (e.g. Zahn et al.,
10   2004b; Hoor et al., 2004; Pan et al., 2004). This mixing reservoir has a variable ventilation regime, with contributions of stratospheric air, UT air and also tropical air masses and exhibits seasonality. There are numerous studies concerning the LMS ventilation (e.g. (Zahn et al., 2004a; Hoor et al., 2005; Pan et al., 2000; Stohl et al., 2003). The range of N_2O between 295 and 320 ppb (Fig. 7) clearly reflects this complex mixing;
15   the variability is indeed visible for different seasons (Fig. 6).

Next we consider the $\delta^{18}O(CO_2)$ data. Whereas CO_2 and $\delta^{13}C(CO_2)$ are inert tracers in the lower stratosphere, $\delta^{17}O(CO_2)$ and $\delta^{18}O(CO_2)$ are not. CO_2 does exchange oxygen isotopes with O_3 due to photochemical interaction via CO_3, which results from excited $O(^1D)$ radicals reacting with CO_2. The isotopic changes are more
20   clearly correlated with N_2O compared to O_3 (Boering et al., 2004), this is valid for N_2O down to 150 ppb. Although the $^{17}O(CO_2)$ increase is closely coupled with $^{18}O(CO_2)$ (Lämmerzahl et al., 2002), $\Delta^{17}O(CO_2)$ is more robust to analytical artifacts and thus better documented. Therefore, to estimate the stratospheric trend (Fig. 7, lower plots), we first use the $\Delta^{17}O(CO_2)$-N_2O trend (Boering et al., 2004), and subsequently the
25   $\Delta^{17}O(CO_2)/\Delta^{18}O(CO_2)$-ratio of 1.7 (Lämmerzahl et al., 2002). The $\delta^{18}O$-N_2O ratio thus constructed characterizes the slope towards low N_2O, taken as 150 ppb.

For fitting CARIBIC-2 observations, the starting point of the stratospheric $\delta^{18}O$-trend was selected to be $\sim$+0.5‰. Overall the CARIBIC-2 data fit the estimated $\delta^{18}O(CO_2)$ trend well (Fig. 7), with negative deviations being expected due to mixing of air masses

having been in contact with surface. Given that our calibration agrees with NOAA (agreement with NIST RMs and NARCIS CO$_2$ was demonstrated by Assonov et al., 2009a, b), the value of +0.5‰ corresponds to a significant contribution of equatorial/tropical air transported to the LMS mixing reservoir (the annual mean in NH tropics, e.g. at MLO over 2001 to 2007 gives +0.49‰). The tropical air contributes to the LMS region by air entering the stratosphere where it resides and certain traces age (also leading to ^{18}O modifications). The (direct) contribution of tropical air to the LMS mixing reservoir via complicated transport is discussed by START group members (e.g. Pan et al., 2009) and would correspond to data points being close to ^{18}O-trend.

Contribution of SH tropical air (which bears positive δ^{18}O(CO$_2$) values, see Fig. 13) to the UT-LMS region in the NH can be excluded on meteorological grounds, and indeed there are only a few positive deviations above the δ^{18}O(CO$_2$) trend given by the line on Fig. 7 (right panel, lower plot). The same is demonstrated by CARIBIC-1 showing more positive deviations vs the trend for SH-affected samples (note that positive values of CARIBIC-1 are reliable). Besides high δ^{18}O(CO$_2$), the FT air masses at low latitudes being affected by SH air have lower CO$_2$ and higher δ^{13}C(CO$_2$). These samples do not contribute to the mixing triangle area (Fig. 7) supporting the δ^{18}O(CO$_2$) picture.

CARIBIC-2 demonstrates numerous deviations below the estimated ^{18}O-trend, thus causing the observed mixing triangle. There is a third component (or components), characterized by high N$_2$O combined with δ^{18}O(CO$_2$) values below 0.5‰, with variable, mostly low CO$_2$. The largest number of samples (highest density of all the triangle areas) appears to have δ^{18}O(CO$_2$) = 0.25‰ and low CO$_2$ with δ^{13}C(CO$_2$) values close to its highest values, around −8.2‰ on the de-trended scale (Fig. 7). At a first glance this may be interpreted as air masses taking part in the UT/LMS mixing, affected by the photosynthetic sink and having being in contact with continental surfaces, which results in lower δ^{18}O(CO$_2$). As candidates of transport we can list fast uplifted (up to 15 km altitude) plumes even crossing the tropopause (e.g. Rhee et al., 2005) as well as isentropic mixing/transport of UT air masses into the LMS (Zahn et al., 2004a) .

Clearly, the new $\delta^{13}C(CO_2)$ and $\delta^{18}O(CO_2)$ data appear to reflect air mixing in the free troposphere and UT/LMS region in a similar way as other tracers such as CO_2, N_2O and SF_6 do. The CO_2 isotope signals in the UT/LMS mixing region resemble signals of tropical air that entered the stratosphere about 2 year prior, accompanied
5 with systematic modifications of $\delta^{18}O(CO_2)$. $\delta^{18}O(CO_2)$ appears to be principally a (new) tracer different from other long lived chemical tracers (such as CO_2, N_2O, SF_6) and also different from $\delta^{13}C(CO_2)$. In the boundary layer $\delta^{18}O(CO_2)$ has a seasonality and a clear latitudinal gradient. Moreover it has a gradient with lower values over the continent's interior (see below). Absent seems to be however a trend in time. There-
10 fore the distribution of $\delta^{18}O(CO_2)$ in the UT/LMS region can be used as independent information to validate descriptions of global transport and UT/LMS mixing in models. Presently the $^{18}O(CO_2)$ "back flux" from the stratosphere is cited as one important un-known in models (Ciais et al., 2005), although proper isotope photochemistry in global circulation models certainly should be able to address this issue. The new data set
15 provides a mean to validate future models. Finally we note that these systematic fea-tures illustrate the successful use of N_2O as a linear tracer of UT/LMS mixing for CO_2, $\delta^{13}C(CO_2)$ and $\delta^{18}O(CO_2)$. Similar plots using the O_3 excess relative to the chemical tropopause level (not shown) show more scatter.

4.2 Variability in CO_2 and $\delta^{13}C(CO_2)$ for FT and UT air masses

20 ### 4.2.1 Latitudinal distribution

For the analysis of tropospheric CO_2 we use the CARIBIC-2 data set (latitudes between 14 and 55°N) because of 3 reasons, being (i) high-resolution sampling; (ii) the data are less affected by de-trending errors; (iii) high quality $\delta^{18}O(CO_2)$ are available for all samples. LMS air masses have been filtered out using the N_2O data.
25 The de-trended CO_2 data demonstrate a surprisingly small gradient over the latitude range 14 to 55°N (Fig. 8). Such was also noticed by analyses of gradients of CO_2

seasonality over NH latitudes (10 to 50 °N, binned in 10° width Schuck et al., 2009). At the surface gradients are caused by especially the large vegetation cover at mid to high latitudes in NH, also resulting in pole-wards increased seasonality (see also surface plots by NOAA (Bowen et al., 2009), also the NOAA web-site). At altitude however, the outflow of the summer monsoon can play a role, be it with a restricted geographical footprint.

UT and FT δ^{13}C(CO$_2$) does not demonstrate a latitudinal gradient, which is anticipated because of the lack of a clear gradient in CO$_2$. This is again in contrast to gradients for surface stations in the NH (plots by NOAA (Bowen et al., 2009), also the NOAA web-site). However the limited number of isotope data we have, precludes us making a detailed analysis as done for the CO$_2$ latitudinal gradient (Schuck et al., 2009) and monsoonal outflow (Schuck et al., 2010). δ^{18}O(CO$_2$) does not show a gradient either meaning that influx of the photochemically driven modification of CO$_2$ is diluted and too small to have an effect for UT air masses. (Note that LMS air may penetrate deeply in the troposphere, here we do not aim to evaluate total UT/LMS budget). Some lower δ^{18}O(CO$_2$) values at 20 to 30°N and, and to a lesser degree at ~50°N indicate fresh plumes that had undergone surface contact in summer (discussed below). A few elevated values for both δ^{13}C(CO$_2$) and δ^{18}O(CO$_2$) in the SH and close to the equator can be understood as the CO$_2$ cycle in the SH differs from that in the NH with high δ^{18}O(CO$_2$) being typical for SH air. The small CARIBIC-1 data set for the SH is also given in Fig. 8 to exemplify typically high SH δ^{18}O(CO$_2$) values.

Concerning N$_2$O the situation is different as it has distinctly lower mixing ratios at high NH latitudes, which is due to the LMS influx of air with lower N$_2$O mixing ratios (discussed in Sect. 4.2.2). In contrast to CO$_2$, N$_2$O seasonality is small and observed variations are mostly due to different air masses crossed, implying this small gradient to be real. Some positive deviations above the main N$_2$O cluster are due to fresh plumes whereas negative ones may indicate the presence of LMS-affected samples not effectively filtered with N$_2$O = 320 ppb. As stratospheric back flux does take place at these latitudes, such air masses do play a role in a total balance.

Analyses of CO$_2$ isotope data for tropical troposphere and UT/LMS

S. S. Assonov et al.

Methane (not shown) has a more or less uniform distribution, with high values at about 20 to 30° N due to monsoon plumes (Schuck et al., 2010). The SF_6 data (not shown) show some scatter due to inhomogeneous distributing of sources located in the NH.

Recapitulating, pertinent features of the latitudinal distributions are: (i) the absence of gradients in CO_2, $\delta^{13}C(CO_2)$ and $\delta^{18}O(CO_2)$ over latitudes of 14 and 55° N. This is in contrast to the clear latitudinal gradient demonstrated by the NOAA NH surface stations accompanied by increased seasonality (see Fig. 13, see also surface plots by NOAA (Bowen et al., 2009), also the NOAA web-site); (ii) the gradient for N_2O, with high latitude values lower by ~0.5 ppb.

4.2.2 Effect of LMS CO_2 on the isotopic composition in the FT and UT

The next issue to address is the effect of the stratosphere-troposphere flux on UT air masses. It has been shown (Nevison et al., 2004, 2007) that the stratospheric influence in the NH significantly contributes to seasonal and inter-annual variations of N_2O and CFC gases with long life times having a strong stratospheric sink. These conclusions are based on surface data, thus an effect at flight altitudes is certainly expected. Although we do not intend to evaluate the total N_2O balance (the LMS-enriched samples are filtered out), one can give some estimation for the dilution brought about by the LMS influx. The N_2O latitudinal gradient (Fig. 8), namely lower N_2O at high NH latitudes implies a contribution of diluted stratospheric air to UT air. We estimate this contribution to be ~2% (latitude gradient of 0.5 ppb and N_2O range in LMS of 25 ppb).

By using the range of CO_2 signals observed over the UT/LMS mixing regime (Fig. 7), the above estimate may be translated for the CO_2 isotope budget. The 2% influence means up to 0.01‰ of unresolved shifts in $\delta^{18}O(CO_2)$, which is well below analytical uncertainty. The effect on $\delta^{13}C(CO_2)$ is even lower, within 0.005‰, and cannot be resolved. Because we have no ^{17}O determination for CO_2, the unavoidable $\delta^{13}C(CO_2)$ analytical artifact/bias arising from stratospheric $^{17}O(CO_2)$ enrichment is about 0.04‰

for the most enriched samples (N_2O about 295 ppb) and is diluted to merely 0.001‰ for the 2% influenced UT-samples. Though these estimations are crude, they show that the stratosphere back flux at high latitudes has negligible effects on ^{13}C and ^{18}O isotope signals in the FT and UT.

4.2.3 Comparison of UT and FT CO_2 isotope data with those from tropical NOAA stations and aircraft

Figure 9 gives the seasonal cycles for free and upper tropospheric CO_2, $\delta^{13}C(CO_2)$ and $\delta^{18}O(CO_2)$ as time series with the CARIBIC data binned in three latitude bands. (The 0 to 20° N band of CARIBIC-2 covers 14 to 20° N.) CARIBIC CO_2 and $\delta^{13}C(CO_2)$ data agree well with those from the selected representative stations the NH tropics (MLO, KUM and IZO) and capture the amplitudes and the seasonality. NOAA stations located at higher latitudes and/or on continents show much larger seasonal variability (MHD is shown as example). Though a certain phase shift between CO_2 data of (marine) boundary layer (selected stations) and signals in FT and UT at the flight altitude can be expected, these aspects are not addressed in this manuscript.

CARIBIC-1 and specifically CARIBIC-2 demonstrate a larger spread of values in each latitude band than results from the aircraft system CONTRAIL (CONTRAIL, 2009) and tropical stations. There may be two separate reasons. For the stations, besides being representative for more homogeneous air masses over the Atlantic, monthly mean values are given. Though CONTRAIL data are based on spot sampling, this project sampled air masses over the Pacific that may have been more homogeneous. CARIBIC sampled air over oceans and continents. Clearly CARIBIC does not demonstrate the strong seasonal amplitudes typical for the NH stations directly affected by continental air masses. Even Mace Head (Fig. 9) which has a limited direct impact of continental air masses compared to truly continental NH stations, demonstrates a much larger seasonal amplitude than CARIBIC.

Regardless the fact that $\delta^{18}O(CO_2)$ is governed by additional processes compared

to CO_2 and $\delta^{13}C(CO_2)$, the similarity between CO_2 and $\delta^{13}C(CO_2)$ of CARIBIC and tropical stations implies the same to be expected for $\delta^{18}O(CO_2)$. We repeat that $\delta^{18}O(CO_2)$ data of CARIBIC-1 demonstrating a large scatter, with variable negative shifts due to CO_2-water exchange in canisters (Assonov et al., 2009b), are used quali-

5 tative only. A few CARIBIC-1 samples exhibit $\delta^{18}O(CO_2)$ values above the trend of the tropical stations. These samples apparently contain SH air where $\delta^{18}O(CO_2)$ values are typically higher than in the NH (Fig. 13, also see below).

The CARIBIC-2 $\delta^{18}O(CO_2)$ values mostly agree with those from tropical stations, although some systematic, mostly negative, deviations occur (Fig. 9). They occur chiefly

10 at latitudes of 14 to 30° N (Fig. 8) (some negative deviations occur also at 40 to 50° N). The deviations in autumn-2008 mainly correspond to monsoon outflow crossed during flights to India. Negative deviations arise from air masses that had been in contact with the surface of continents where intensive ^{18}O exchange with soil and leaf water takes place (Ciais et al., 1997). Such CARIBIC-2 signals are similar to (but more positive

15 than) the data of Mace Head, a station affected both by marine and continental air. With Mace Head being at mid latitudes, $\delta^{18}O$ values of precipitation and soil water are lower than in the tropics. Positive $\delta^{18}O(CO_2)$ values of CARIBIC-2 (years 2008 and 2009) of up to 1.0‰ correspond to samples containing SH air which bears more positive $\delta^{18}O(CO_2)$ values (see also Fig. 13) due to the much smaller land cover. Positive

20 values were also observed by CARIBIC-1 close to the equator and in the SH (Fig. 8).

4.2.4 Carbon cycle and isotope signals

To better understand signals observed by CARIBIC, we briefly summarize the carbon cycle. In the troposphere CO_2 concentration and $\delta^{13}C(CO_2)$ reflect the variability, both in time and space, of CO_2 sources and sinks (respiration, photosynthesis, ocean

25 uptake, fossil fuel and biomass burning). As source and sink processes cause isotope fractionation, variations in CO_2 and $\delta^{13}C(CO_2)$ are closely linked and largely in anti-phase. Photosynthesis produces biomass depleted in ^{13}C with remaining air CO_2

becoming enriched (e.g. Bowling et al., 2008).

One can presume that respiration, and combustion of fossil fuel and biomass accumulated by photosynthesis will tend to bring air $\delta^{13}C(CO_2)$ back to initial values. This is only partly true because of a disequilibrium effect – recently formed biomass is linked (by overall photosynthesis fractionation) to modern air $\delta^{13}C(CO_2)$ (around -8.3‰), whereas part of respiration and all combustion releases carbon accumulated in the past when $\delta^{13}C(CO_2)$ was higher by up to about 2‰ (Francey et al., 1999).

Anthropogenic effects on the CO_2 cycle include fossil fuel burning, increased biomass burning, change of land use, deforestation, erosion, cement production etc. Fossil fuel carbon is characterized by negative $\delta^{13}C(CO_2)$, e.g. around –24‰ for coal, oil from –30 to –26‰, combustion of natural gas mix (biogenic and thermogenic methane) of ~ -44‰ (e.g. Ciais et al., 1995 and references therein). On the average fossil fuel has a $\delta^{13}C(CO_2)$ value of about –28‰, being close to an overall old biomass signature.

The gross ocean fluxes exceed the net uptake many times. Ocean uptake has a disequilibrium effect of the same nature as outlined above for photosynthesis – the dissolved CO_2 pool has been in equilibrium with the atmosphere for a long time, when atmospheric $\delta^{13}C(CO_2)$ was higher. Thus the exchange back-flux from the ocean returns CO_2 with $\delta^{13}C(CO_2)$ values higher than the value of the modern CO_2 uptake (e.g. Quay et al., 2003).

The important CO_2 sources and sinks of different $\delta^{13}C(CO_2)$ signatures can be traced by using Keeling plots, which are based on the assumption of the admixture of air with CO_2 affected by source and sink processes to background air e.g. (Pataki et al., 2003; Miller et al., 2003). As sources and sinks are unequally distributed over the globe and have different seasonality the intercept values on Keeling plot are variable.

4.2.5 Variability in CO$_2$ and δ^{13}C(CO$_2$) of FT and UT air masses

Despite the long distances covered during a single CARIBIC flight (up to 8000 km), good, at times excellent, correlations between δ^{13}C(CO$_2$) and CO$_2$ are evident for many flights (Fig. 10, upper panel). As best example we give the flight Frankfurt-Toronto-Frankfurt on 17–18 September 2007 with sampling latitudes from 43 to 53° N and 8 day back trajectories reaching from 20 to 70° N. After filtering out the LMS contribution using N$_2$O as elucidated before, GHG and other tracers confirm that we are dealing with pure FT and UT air masses. These tropospheric air masses were nevertheless of variable origin and history and for instance CH$_4$ showed considerable variability. However, δ^{13}C(CO$_2$) correlates extremely well with CO$_2$ over the 8000 km flight route. The isotope data reveal this behavior for ^{13}C within a total range of merely ~0.1‰ thanks to their high precision. This snapshot of a single flight demonstrates large scale similarities of source and sink processes.

We emphasize that the compact correlations during single flights reflect behavior for air masses during specific seasons. It is clear that the relationship changes during the seasons (Fig. 10, lower panel). Winter and summer correlations demonstrate statistically different intercept values (from –29 to –24‰, Fig. 10, lower panel) due to the variable balance of CO$_2$ sources and sinks for different seasons.

Although a similarity between CO$_2$ and δ^{13}C(CO$_2$) for the CARIBIC time series and data for NH tropical stations (Fig. 9, see above) is observed, the variability of CO$_2$ and δ^{13}C(CO$_2$), even during a single flight, is large. The reasons for this can be explored by using Keeling plots. When δ^{13}C(CO$_2$) data of CARIBIC-1 (only lat >14° N) and CARIBIC-2 data are plotted vs. the inverse of the CO$_2$ mixing ratio (Fig. 11), nearly all CARIBIC samples are within the amplitude range demonstrated by tropical stations (plotted are data for KUM). The shift between CARIBIC-1 and CARIBIC-2 data clusters agrees with the global trend demonstrated by background/remote stations MLO and KUM. The intercept of the stations' trend (the value of ~–14‰, see Sect. 3.2), mainly characterizes the global CO$_2$ trend.

Only few CARIBIC data points reach beyond the range of MLO and KUM (Fig. 11). Low values indicate more pronounced effects from respiration, fossil fuel and biomass burning. High δ^{13}C(CO$_2$) values are indicative for a large impact of photosynthesis (contributions of SH air cannot be excluded either). The amplitude of variations for CARIBIC is, as expected, much less than that for the stations affected by continental air masses, e.g. MHD.

The CARIBIC clusters appear to demonstrate a fine structure with the variability in δ^{13}C(CO$_2$) and CO$_2$ being closely correlated. The slope is similar to that of the annual cycle at any NH station with pronounced seasonality, e.g. at MHD (Fig. 11). Trends observed over particular flights and also over seasons (Fig. 10) are already within this structure; on this plot (data not de-trended) the variability of seasonal slopes is practically indistinguishable. Thus, along the seasonal variability demonstrated by stationary stations in NH tropics, another important reason for correlated variability in δ^{13}C(CO$_2$) and CO$_2$ detected by the aircraft platform is the variability in FT and UT air masses crossed. The fact that variability for high resolution sampling is much larger (see Fig. 9) confirms this. One reason for pronounced variability is that at times fresh plumes are intersected. For instance flights 186 to 189 crossed biomass burning plumes over China (Lai et al., 2010). The data demonstrate some correlations between increases in CO and CO$_2$ and negative shifts in δ^{13}C(CO$_2$). Monsoon plumes were also crossed which were identified by increases in methane and some (negative) δ^{18}O(CO$_2$) shifts, without clear effects for δ^{13}C(CO$_2$).

We interpret the correlated variability in δ^{13}C(CO$_2$) and CO$_2$ (Fig. 12) as result of mixing of masses affected to different degrees by seasonally varying sources and sinks with well-mixed background air masses. In first approximation, the overall effect of all major (global) sources and sinks result in the same slope of isotope fractionation. Thus correlations in δ^{13}C(CO$_2$) and CO$_2$ in FT and UT air over a hemisphere are rather a rule than exception and reflect the global CO$_2$ cycle in the NH. The figure shows compact correlations for the de-trended CARIBIC-1 and CARIBIC-2 data sets for all seasons. The two data sets cover basically the same range of values, with nearly

identical slopes and intercepts. Most obvious deviations due to SH air admixture (as inferred by positive deviations in $\delta^{18}O(CO_2)$) have been filtered out. As we have no robust chemical tracer for SH air, some outliers due to SH air cannot be excluded. Obviously, the deviations from the fit lines exceed deviations observed for particular

5 seasonal trends as the year-around variability includes several seasonal effects which give variable trends (intercepts from −29 to −24‰, Fig. 10).

All in all, the variability of signals is both due to mixing of different air masses affected by sources and sinks (the matter of atmospheric transport) and the seasonal variability of sources and sinks in the NH. On top of this there is the variability due to UT/LMS

10 mixing; the latter is well recognized by using stratospheric tracers. We note that the use of isotopes directly reveals the causes for CO_2 variability. Without isotopes, one may imply rather a similarity of air masses in the FT and UT or data scatter (Schuck et al., 2009). However explaining/describing CO_2 and isotope signals of the FT and UT region in detail is not trivial and will require advanced coupled biosphere-ocean-atmosphere

15 models.

4.2.6 Variability in tropospheric $\delta^{18}O(CO_2)$

Of overriding importance for $\delta^{18}O(CO_2)$ and its variations is ^{18}O exchange with water (leaf, soil, and ocean water) via bicarbonate formation. The isotope change depends directly on the $\delta^{18}O(H_2O)$ value while the fractionation constant possesses a strong

20 temperature dependence (Brenninkmeijer et al., 1983). The variations in $\delta^{18}O(CO_2)$ cannot be detected by the Keeling plot technique, which is based on the assumption of mixing. Only combustion acts as a source in that sense. However fossil fuel and biomass burning combustion constitute a small flux compared to the gross CO_2 fluxes whereby CO_2 undergoes ^{18}O exchange. Consequently, $\delta^{18}O(CO_2)$ is a specific tracer

25 of gross CO_2 fluxes. Accurate measurements of $\delta^{18}O(CO_2)$ on a large scale started only years ago and not much data interpretation is available; understanding ecosystem-atmosphere exchange processes is underway, e.g. (Still et al., 2009). We also reiterate

that $\delta^{18}O(CO_2)$ is a tracer of air transport and mixing as we demonstrated for the UT/LMS region.

The similarity between $\delta^{13}C(CO_2)$ and CO_2 of CARIBIC and the data of representative stations in the NH tropical boundary layer implies the same similarity to be expected for $\delta^{18}O(CO_2)$. At a first glance (Fig. 9), $\delta^{18}O(CO_2)$ of CARIBIC-1 and CARIBIC-2 demonstrates a scatter, with many negative deviations versus the tropical stations' trend. When plotting $\delta^{18}O(CO_2)$ versus CO_2, no structure is discernable (plot not given). The year 2008 demonstrates a larger variability than 2007, due to different routes and the Indian summer monsoon.

The NOAA data help understanding characteristics of the $\delta^{18}O(CO_2)$ patterns. First, the amplitude of the $\delta^{18}O(CO_2)$ seasonal cycle systematically increases from the SH to high NH latitudes whereas the annual means decrease (Fig. 13, upper panel). Besides this SH-NH gradient due to the NH land masses, there also are significant gradients across continents. The actual $\delta^{18}O(CO_2)$ values depend on $\delta^{18}O$ of precipitation, temperature, evaporation and evapotranspiration (see e.g. plots in Ciais et al., 1997). The largest $\delta^{18}O(CO_2)$ seasonal cycle in the NH can be best illustrated by the gradient between MLO and Barrow data (Fig. 13, upper panel).

As the exchange with water vapor in air is negligible and $\delta^{18}O(CO_2)$ is only affected by dilution with background air, the largest $\delta^{18}O(CO_2)$ variability can be expected in fresh plumes. Indeed, the most prominent negative $\delta^{18}O(CO_2)$ shifts are in autumn 2008 (Fig. 9) for the flights to India and China in 2008 which crossed large plumes of surface air (August to December).

Besides negative deviations from the trend of NH tropic stations, there are some positive deviations. The highest $\delta^{18}O(CO_2)$ values are around +0.9‰ in November–December 2008 at about 20° N (Fig. 9) which are expected to have been due to significant contributions of SH air with high $\delta^{18}O(CO_2)$ values (Fig. 13). In fact high values (around +1.0‰) were also recorded by samples taken close to equator and in SH (African flights) by CARIBIC-1 (3 March 2000) and CARIBIC-2 (10 to 12 March 2009) (Fig. 8).

Title Page

Abstract | Introduction

Conclusions | References

Tables | Figures

◄ | ►

◄ | ►

Back | Close

Full Screen / Esc

Printer-friendly Version

Interactive Discussion

4.3 Signals recorded by CARIBIC in the FT and UT and global atmospheric circulation

Next we revisit the latitudinal distribution of CO_2 (Fig. 8). To understand the latitudinal distribution of the CONTRAIL aircraft CO_2 data (Matsueda et al., 2002, 2008) obtained at similar flight altitudes, Miyazaki et al. (2008, 2009) applied a global atmospheric transport model. They concluded, we cite (Miyazaki et al., 2009): "In the NH subtropical upper troposphere, the formation of the latitudinal CO_2 gradient is mostly attributable to the upward and poleward (adiabatic) transports of CO_2...." Based on their model results, the CO_2 concentration gradient at flight altitudes of 300 to 200 hPa is very limited or, in some months, negligible. That is basically in agreement with the similarity of the range of CO_2 and isotope signals over the corresponding NH latitudes observed by CARIBIC (Fig. 8).

The strongest gradient in the CO_2 latitudinal distribution at flight altitudes appears in summer, at latitudes 45 to 75° N (Fig. 5 in (Miyazaki et al., 2008) and also Fig. 3 in (Miyazaki et al., 2009). These latitudes are expected to have lower UT CO_2 due to uplift of strongly depleted continental air in summer. Though the model of (Miyazaki et al., 2008, 2009) does not include the stratospheric flux at mid-latitudes, the effect on concentrations (not directly in UT/LMS structures) cannot be large, about 2% of the maximal LMS/UT variability (Sect. 4.2.2) which is translated to up to some 0.2 ppm. The model results by (Shia et al., 2006) show that cross-tropopause exchange is pronounced in certain seasons, but the results do not allow to evaluate this contribution correctly. A recent study by (Boenisch et al., 2008) aimed to model CO_2 and SF_6 in the extratropical UT/LS, including STE flux, has demonstrated little gradient at the CARIBIC flight altitudes in the NH latitudes (14 to 55° N), also with an increased gradient in summer.

At last, based on de-trended data, we evaluate the seasonal cycle of $\delta^{13}C(CO_2)$ and CO_2 in the FT and UT. CARIBIC-1 and CARIBIC-2 data demonstrate basically the same seasonality and amplitude (Fig. 14, our final figure, left panel). This agreement

shows the data to be representative and to be of high quality. Noting that CARIBIC-1 and CARIBIC-2 have different flight routes, that measurements were performed by different sampling and extraction systems, in two different labs, with a time lag of 5 years give confidence that isotope data of required precision and accuracy can be obtained.

After filtering out data of fresh plumes (by total H_2O above 2000 ppb and CO above 125 ppb, only a few data points), the FT plus UT data are in line with the phase and the range of values at the NOAA stations in the NH tropics (Fig. 14, right panel). As CARIBIC is a moving platform, it demonstrates higher variability than selected tropical stations sampling only representative air masses. The variability of FT +UT signals at flight altitudes is due to mixing of air masses affected by sources and sinks with background air; the effect of UT/LMS mixing is limited. Averaged values observed by CARIBC-2 and presented by using the box plot (Fig. 14, right panel) can in first instance be considered as monthly values of background air in FT and UT. The agreement with the data of NOAA stations in NH tropics supports the hypothesis of uplift and transport of tropical air.

Overall we conclude that general features demonstrated by CO_2 and its isotope signals of CARIBIC appear to agree with expectations based on general atmospheric circulation. However at the moment there are few models which implement all details of global circulation, and adequately describe CO_2 sources and sinks, etc.

4.4 Variability of CO_2 signals and analytical errors – where is the optimal resolution?

At cruise altitudes, the variability detected in FT and UT air masses (de-trended data) is about 10 ppm for CO_2 and 0.4‰ for $\delta^{13}C(CO_2)$. Given that total combined uncertainty we have reached are respectively 0.2 ppm and 0.02‰ (1-σ values, that is, a 20 ppm variation in the $\sim$1.1% ^{13}C in carbon), this translates into 2% and 5% relative variability. This is a rather reasonable balance between signals and errors. The correlations observed between CO_2 and $\delta^{13}C(CO_2)$ (e.g. Fig. 10) imply that at the moment actual

analytical errors in CO_2 and $\delta^{13}C(CO_2)$ (at the level of our laboratory performance) are rather well balanced.

We stress that for meaningful use of such data in models, data merging from different laboratories is critical. The only inter-laboratory comparison performed was with
5 MPI-BGC, Jena, during which the discrepancies of 0.04 and 0.07‰ for $\delta^{13}C(CO_2)$ and $\delta^{18}O(CO_2)$ were documented (Assonov et al., 2009a). Although this exceeds the 1-sigma errors evaluated by the two labs and exceeds the $\delta^{13}C(CO_2)$ data comparability target of merging data from different laboratories (13th_WMO/IAEA_Meeting, Expert Group Recommendations), inter-laboratory scale discrepancies observed by
10 round robins among other labs are unfortunately much larger (Levin et al., 2007). Importantly, the offset between MPI-BGC and NOAA being documented is limited and stable in time, permitting to reconstruct a (possible) offset between the NOAA scale realization and that of CARIBIC.

4.5 Future use of data, optimal sampling resolution and other aspects

15 When one intends to obtain representative information on the global CO_2 cycle by using limited capabilities, optimizing sampling strategy is needed. In our case, optimal flight frequency, the distance covered by a single sample, and the sampling frequency need consideration. On the one hand, sampling at low resolution, similar to that of most models is logical. High-resolution sampling gives a more detailed picture of mixing
20 effects and structures involved, but the information, given a certain sample capacity is reduced.

Comparing CARIBIC-1 and CARIBIC-2 data in this context gives useful information. Obviously the high sampling resolution by CARIBIC-2 (15 km of flight distance per sample) with 28 samples per outward and return flights gives a different picture
25 than obtained by the low resolution of CARIBIC-1 (~250 km per sample, 12 samples per flight). This is well illustrated by the UT/LMS mixing trends. CARIBIC-2 clearly demonstrates the L-shape mixing in the UT/LMS region being visible both for

Analyses of CO_2 isotope data for tropical troposphere and UT/LMS

S. S. Assonov et al.

Title Page

Abstract	Introduction
Conclusions	References
Tables	Figures

◄◄ ►►

◄ ►

Back Close

Full Screen / Esc

Printer-friendly Version

Interactive Discussion

δ^{13}C(CO$_2$) and δ^{18}O(CO$_2$). Occasionally δ^{18}O(CO$_2$) shows even more regular patterns than δ^{13}C(CO$_2$). In contrast, UT/LMS data by CARIBIC-1 show only linear trends for δ^{13}C(CO$_2$) without details or systematic pattern for δ^{18}O(CO$_2$). (Some CARIBIC-1 trends are given in Assonov et al., 2007). This is partly because of the inferior δ^{18}O(CO$_2$) data quality and resolution of CARIBIC-1. Low and high resolution sampling give different data sets. When frequent tropopause crossings occur at mid latitudes, a higher resolution may be preferable.

5 Summary and outlook

1. CARIBIC provided unique isotope data sets for the UT/LMS and free tropical troposphere, with about ∼1 month resolution. CARIBIC-1 (1999 to April 2002), with low resolution sampling (250 km/per sample) provided high quality δ^{13}C(CO$_2$) data and lower quality δ^{18}O(CO$_2$). CARIBIC-2 (April 2007–March 2009) provided accurate and reliable δ^{13}C(CO$_2$) and δ^{18}O(CO$_2$) data on high-resolution sampling (about 15 km/sample). For all samples extensive supporting GHG, O$_3$, CO and meteorological data are available.

2. The manuscript presents the first analyses of the CARIBIC-2 data for tracer-tracer correlations, distribution and trends with detailed information for UT/LMS CO$_2$, δ^{13}C(CO$_2$) and δ^{18}O(CO$_2$). For the first time it is demonstrated that global-scale variability in air mass origin and GHG signals are reflected by the variability in δ^{13}C(CO$_2$) and δ^{18}O(CO$_2$). Besides the UT/LMS mixing, such correlations arise from different degrees of mixing of background air with air masses affected by sources and sinks, over the distance up to 8000 km and also over different seasons. The trends and features demonstrated by CARIBIC-2 are found to agree with CARIBIC-1 signals attenuated over long sampling distance, except of δ^{18}O(CO$_2$).

3. Data de-trending and use of stratospheric tracers is considered. We demonstrate that N_2O is the most adequate tracer in describing CO_2 signals in the UT/LMS region. By filtering out LMS data (using N_2O as stratospheric tracer) and data of fresh plumes, data for FT and UT background air masses were obtained. The data and trends agree well with the data of NOAA stations in NH tropics. This is in agreement with global atmospheric transport with the uplift and transport of tropical air masses pole-wards.

4. The $\delta^{18}O(CO_2)$ data are discussed to reflect air mixing in the FT and UT/LMS region. $\delta^{18}O(CO_2)$ appears to be a principally different tracer than other long lived chemical tracers (such as CO_2, N_2O, SF_6) as it has both a seasonality and clear latitudinal gradient, in the absence of a trend in time. Therefore the distribution of $\delta^{18}O(CO_2)$ in the UT/LMS region can be used as independent tracer to validate description of global transport and UT/LMS mixing in models.

5. Climate change will most likely show up in $\delta^{18}O(CO_2)$. Although it is a highly complex signal, its link to temperature, humidity, soils and vegetation makes it desirable to monitor $\delta^{18}O(CO_2)$ not only at the surface but also at altitude. Thereafter obtained present-day record for the FT and UT/LMS region is an asset to future comparisons.

6. Considering future developments of observations by aircraft, sampling resolution and optimal analytical uncertainty are critical. While high-resolution sampling is extremely valuable to study effects in detail UT/LMS mixing and inter-hemispheric transport, it may be less applicable when one aims obtaining representative signals for remote FT and UT on the global scale for use in models.

7. The data shown are based on a major research effort (made possible by IRMM in Geel, Belgium for CARIBIC-2), that could not be sustained at present but should be taken up again in the not too distant future. An 88 sampling system

in CARIBIC-2, to operate in addition to the 28 sample system is close to completion and should be deployed early 2010.

8. Though the CARIBIC data set is self-consistent, inter-laboratory consistency for CO_2 isotope data aimed future data merging may be a limiting issue in the future. The calibration scale used for CARIBIC-1 and -2 was verified by agreement with NIST RMs and Narciss CO_2 gases. A scale discrepancy between IRMM and MPI-BGC was documented, which is small compared to scale discrepancies documented otherwise.

Appendix A

Abbreviations

CARIBIC – Civil Aircraft for the Regular Investigation of the atmosphere Based on an Instrument Container, www.caribic-atmospheric.com
　FT – free troposphere
　LMS – lowermost stratosphere
　LS – lower stratosphere
　NH – Northern Hemisphere
　STE – stratosphere-troposphere exchange
　SH – Southern Hemisphere
　UT – upper troposphere
　UTLS – upper troposphere-lowermost stratosphere

NOAA stations are given by using the following abbreviations:

AZR – Terceira Island, Azores, Portugal, 38.77 N; 27.38 W; 40 m a.s.l.;
KUM – Cape Kumukahi, Hawaii, United States, 19.52 N; 154.82 W; 3 m a.s.l.;

IZO – Tenerife, Canary Islands, Spain, 28.3 N, 16.48 W; 2360 m a.s.l.;
MHD – Mace Head, Ireland, 53.33 N; 9.9 W; 25 m a.s.l.;
MID – Sand Island, Midway, United States, 28.21 N; 177.38 W; 7.7 m a.s.l.;
MLO – Mauna Loa, Hawaii, United States, 19.54 N, 155.58 W; 3397 m a.s.l..

References

Allison, C. E., Francey, R. J., and Meijer, H. A. J.: Recommendation for the reporting of stable isotope measurements of carbon and oxygen in CO_2 gas., IAEA-TECDOC-825, Vienna, IAEA-TECDOC-825, 155–162, 1995.

Andrews, A. E., Boering, K. A., Daube, B. C., Wofsy, S. C., Loewenstein, M., Jost, H., Podolske, J. R., Webster, C. R., Herman, R. L., Scott, D. C., Flesch, G. J., Moyer, E. J., Elkins, J. W., Dutton, G. S., Hurst, D. F., Moore, F. L., Ray, E. A., Romashkin, P. A., and Strahan, S. E.: Mean ages of stratospheric air derived from in situ observations of CO_2, CH_4, and N_2O, J. Geophys. Res.-Atmos., 106, 32295–32314, 2001.

Assonov, S., Taylor, P., and Brenninkmeijer, C. A. M.: A system for high-quality CO_2 isotope

Title Page

Abstract | Introduction

Conclusions | References

Tables | Figures

◄ | ►

◄ | ►

Back | Close

Full Screen / Esc

Printer-friendly Version

Interactive Discussion

analyses of air samples collected by the CARIBIC Airbus A340-600, Rapid Commun. Mass Spectrom., 23, 1347–1363, 2009a.

Assonov, S. S. and Brenninkmeijer, C. A. M.: A re-determination of absolute values for $^{17}R_{VPDB-CO_2}$ and $^{17}R_{VSMOW}$, Rapid Commun. Mass Spectrom., 17, 1017–1029, 2003.

Assonov, S. S., Brenninkmeijer, C. A. M., Zahn, A., and Koeppel, C.: CO_2 isotopic composition in the upper troposphere: the project CARIBIC, 14th WMO/IAEA Meeting of Experts on Carbon Dioxide Concentration and Related Tracers Measurement Techniques, Helsinki, Finnland, 9–22 September 2007, 2007.

Assonov, S. S., Brenninkmeijer, C. A. M., Koeppel, C., and Röckmann, T.: CO_2 isotope analyses using large air samples collected on intercontinental flights by the CARIBIC Boeing 767, Rapid Commun. Mass Spectrom., 23, 822–830, 2009b.

Bender, M. L., Ho, D. T., Hendricks, M. B., Mika, R., Battle, M. O., Tans, P. P., Conway, T. J., Sturtevant, B., and Cassar, N.: Atmospheric O_2/N_2 changes, 1993-2002: Implications for the partitioning of fossil fuel CO_2 sequestration, Global Biogeochem. Cy., 19, GB4017, doi:10.1029/2004gb002410, 2005.

Bischof, W. and Bolin, B.: Space and time variations of CO_2 content of troposphere and lower stratosphere, Tellus, 18, 155–159, 1966.

Boenisch, H., Hoor, P., Gurk, C., Feng, W., Chipperfield, M., Engel, A., and Bregman, B.: Model evaluation of CO_2 and SF_6 in the extratropical UT/LS region, J. Geophys. Res., 113, D06101, doi:10.1029/2007JD008829, 2008.

Boering, K. A., Jackson, T., Hoag, K. J., Cole, A. S., Perri, M. J., Thiemens, M., and Atlas, E.: Observations of the anomalous oxygen isotopic composition of carbon dioxide in the lower stratosphere and the flux of the anomaly to the troposphere, Geophys. Res. Lett., 31, L03109, doi:03110.01029/02003GL018451, 2004.

Bowen, G. J., West, J. B., Vaughn, B. H., Dawson, T. E., Ehleringer, J. R., Fogel, M. L., Hobson, K., Hoogewerff, J., Kendall, C., Lai, C.-T., Miller, C. C., Noone, D., Schwarcz, H., and Still, C. J.: Isoscapes to Address Large-Scale Earth Science Challenges, EOS, Transactions American Geophysical Union, 90(13), 109–110, doi:10.1029/2009EO130001, 2009.

Bowling, D. R., Pataki, D. E., and Randerson, J. T.: Carbon isotopes in terrestrial ecosystem pools and CO_2 fluxes, New Phytol., 178, 24–40, 2008.

Brand, W. A., Assonov, S. S., and Coplen, T. B.: Correction for the ^{17}O interference in $\delta^{13}C$ measurements when analyzing CO_2 with stable isotope mass spectrometry, Pure Anal. Chem., submitted, 2009.

Analyses of CO_2 isotope data for tropical troposphere and UT/LMS

S. S. Assonov et al.

Brenninkmeijer, C. A. M., Kraft, P., and Mook, W. G.: Oxygen Isotope Fractionation Between CO_2 and H_2O, Isotope Geoscience, 1, 181–190, 1983.

Brenninkmeijer, C. A. M., Crutzen, P. J., Fischer, H., Gusten, H., Hans, W., Heinrich, G., Heintzenberg, J., Hermann, M., Immelmann, T., Kersting, D., Maiss, M., Nolle, M., Pitscheider, A., Pohlkamp, H., Scharffe, D., Specht, K., and Wiedensohler, A.: CARIBIC - Civil aircraft for global measurement of trace gases and aerosols in the tropopause region, J. Atmos. Ocean. Technol., 16, 1373–1383, 1999.

Brenninkmeijer, C. A. M., Crutzen, P., Boumard, F., Dauer, T., Dix, B., Ebinghaus, R., Filippi, D., Fischer, H., Franke, H., Frieß, U., Heintzenberg, J., Helleis, F., Hermann, M., Kock, H. H., Koeppel, C., Lelieveld, J., Leuenberger, M., Martinsson, B. G., Miemczyk, S., Moret, H. P., Nguyen, H. N., Nyfeler, P., Oram, D., O'Sullivan, D., Penkett, S., Platt, U., Pupek, M., Ramonet, M., Randa, B., Reichelt, M., Rhee, T. S., Rohwer, J., Rosenfeld, K., Scharffe, D., Schlager, H., Schumann, U., Slemr, F., Sprung, D., Stock, P., Thaler, R., Valentino, F., Van Velthoven, P., Waibel, A., Wandel, A., Waschitschek, K., Wiedensohler, A., Xueref-Remy, I., Zahn, A., Zech, U., and Ziereis, H.: Civil Aircraft for the regular investigation of the atmosphere based on an instrumented container: The new CARIBIC system, Atmos. Chem. Phys., 7, 4953–4976, 2007, http://www.atmos-chem-phys.net/7/4953/2007/.

Callendar, G. S.: The Artificial Production of Carbon Dioxide and Its Influence on Temperature, Q. J. Roy. Meteorol. Soc., 64, 223–240, 1938.

Ciais, P., Tans, P. P., White, J. W. C., Trolier, M., Francey, R. J., Berry, J. A., Randall, D. R., Sellers, P. J., Collatz, J. G., and Schimel, D. S.: Partitioning of Ocean and Land Uptake of CO_2 as Inferred by Delta-C-13 Measurements from the NOAA Climate Monitoring and Diagnostics Laboratory Global Air Sampling Network, J. Geophys. Res.-Atmos., 100, 5051–5070, 1995.

Ciais, P., Denning, A. S., Tans, P. P., Berry, J. A., Randall, D. A., Collatz, G. J., Sellers, P. J., White, J. W. C., Trolier, M., Meijer, H. A. J., Francey, R. J., Monfray, P., and Heimann, M.: A three-dimensional synthesis study of $\delta^{18}O$ in atmospheric CO_2. 1. Surface fluxes, J. Geophys. Res.-Atmos., 102, 5857–5872, 1997.

Ciais, P., Cuntz, M., Scholze, M., Mouillot, F., Peylin, P., and Gitz, V.: Remarks on the use of 13C and 18O isotopes in Atmospheric CO_2 to Quantify biospheric carbon fluxes, in: Stable Isotopes and Biosphere Atmosphere Interactions, Academic Press, San Diego, CA, USA, 235–267, 2005.

CONTRAIL 2009: CO_2 flask event Comprehensive Observation Network for TRace gases by

AIrLiner (CONTRAIL), Period 1993-04-23 to 2007-12-20, Version 2008-08-05, available on-line at: http://gaw.kishou.go.jp/, 2009.

Dlugokencky, E. J., Steele, L. P., Lang, P. M., and Masarie, K. A.: The growth rate and distribution of atmospheric methane, J. Geophys. Res., 99, 17021–17043, 1994.

Engel, A., Mobius, T., Bonisch, H., Schmidt, U., Heinz, R., Levin, I., Atlas, E., Aoki, S., Nakazawa, T., Sugawara, S., Moore, F., Hurst, D., Elkins, J., Schauffler, S., Andrews, A., and Boering, K.: Age of stratospheric air unchanged within uncertainties over the past 30 years, Nature Geosci, 2, 28–31, 2009.

Francey, R. J., Allison, C. E., Etheridge, D. M., Trudinger, C. M., Enting, I. G., Leuenberger, M., Langenfelds, R. L., Michel, E., and Steele, L. P.: A 1000-year high precision record of δ^{13}C in atmospheric CO_2, Tellus, 51B, 170–193, 1999.

GLOBALVIEW-CO_2: Cooperative Atmospheric Data Integration Project – Carbon Dioxide. CD-ROM, NOAA ESRL, Boulder, Colorado, online available via anonymous ftp to ftp.cmdl.noaa.gov, path: ccg/co2/GLOBALVIEW, 2009.

GLOBALVIEW-CO_2C13: Cooperative Atmospheric Data Integration Project – d^{13}C of Carbon Dioxide. CD-ROM, NOAA ESRL, Boulder, Colorado, online available via anonymous ftp to ftp.cmdl.noaa.gov, path: ccg/co2c13/GLOBALVIEW, 2009.

Hall, T. M., Waugh, D. W., Boering, K. A., and Plumb, R. A.: Evaluation of transport in stratospheric models, J. Geophys. Res.-Atmos., 104, 18815–18839, 1999.

Hegglin, M. I. and Shepherd, T. G.: O_3-N_2O correlations from the Atmospheric Chemistry Experiment: Revisiting a diagnostic of transport and chemistry in the stratosphere, J. Geophys. Res., 112, D19301, doi:10.1029/2006jd008281, 2007.

Hoor, P., Gurk, C., Brunner, D., Hegglin, M. I., Wernli, H., and Fischer, H.: Seasonality and extent of extratropical TST derived from in-situ CO measurements during SPURT, Atmos. Chem. Phys., 4, 1427–1442, 2004, http://www.atmos-chem-phys.net/4/1427/2004/.

Hoor, P., Fischer, H., and Lelieveld, J.: Tropical and extratropical tropospheric air in the low-ermost stratosphere over Europe: A CO-based budget, Geophys. Res. Lett., 32, L07802, doi:07810.01029/02004GL022018, 2005.

Jiang, X., Ku, W. L., Shia, R.-L., Li, Q., Elkins, J. W., Prinn, R. G., and Yung, Y. L.: Seasonal cycle of N2O: Analysis of data, Global Biogeochem. Cy., 21, GB1006, doi:10.1029/2006gb002691, 2007.

Keeling, C. D.: The concentration and isotopic abundances of carbon dioxide in rural and marine air, Geochim. Cosmochim. Acta, 24, 277–298, 1961.

Analyses of CO_2 isotope data for tropical troposphere and UT/LMS

S. S. Assonov et al.

Title Page

Abstract	Introduction
Conclusions	References
Tables	Figures

|◄ | ►|

◄ | ►

Back | Close

Full Screen / Esc

Printer-friendly Version

Interactive Discussion

Köppe, M., Hermann, M., Brenninkmeijer, C. A. M., Heintzenberg, J., Schlager, H., Schuck, T., Slemr, F., Sprung, D., van Velthoven, P. F. J., Wiedensohler, A., Zahn, A., and Ziereis, H.: Origin of aerosol particles in the mid latitude and subtropical upper troposphere and lowermost stratosphere from cluster analysis of CARIBIC data, Atmos. Chem. Phys., 9, 8413–8430, 2009, http://www.atmos-chem-phys.net/9/8413/2009/.

Lai, S. C., Baker, A. K., Schuck, T. J., van Velthoven, P., Oram, D. E., Zahn, A., Hermann, M., Weigelt, A., Slemr, F., Brenninkmeijer, C. A. M., and Ziereis, H.: Pollution events observed during CARIBIC flights in the upper troposphere between South China and the Philippines, Atmos. Chem. Phys., 10, 1649–1660, 2010, http://www.atmos-chem-phys.net/10/1649/2010/.

Lämmerzahl, P., Röckmann, T., Brenninkmeijer, C. A. M., Krankowsky, D., and Mauersberger, K.: Oxygen isotope composition of stratospheric carbon dioxide, Geophys. Res. Lett., 29, 1582, doi:1510.1029/2001GL014343, 2002.

Levin, I., Allison, C., Brand, W., Conway, Delmotte, M., Facklam, C., Francey, R., Hammer, S., Huang, L., Jordan, A., Langenfelds, R., Machida, T., Meijer, H., Mukai, H., Neubert, R., Sabasch, M., Schmidt, M., Steele, P., Steinberg, B., Ramonet, M., Rothe, M., Vaughn, B., and Worthy, D.: Five Years of International Flask Intercomparison (Sausage Flask ICP) 2002-2007, 14th WMO/IAEA Meeting of Experts on Carbon Dioxide Concentration and Related Tracers Measurement Techniques, Helsinki, Finland, 10–13 September 2007, 2007.

Levin, I. and Karstens, U.: Inferring high-resolution fossil fuel CO2 records at continental sites from combined $^{14}CO_2$ and CO observations, Tellus B – Chem. Phys. Meteorol., 59, 245–250, 2007.

Levin, I., Hammer, S., Kromer, B., and Meinhardt, F.: Radiocarbon observations in atmospheric CO2: Determining fossil fuel CO_2 over Europe using Jungfraujoch observations as background, Sci. Total Environ., 391, 211–216, 10.1016/j.scitotenv.2007.10.019, 2008.

Lintner, B. R., Buermann, W., Koven, C. D., and Fung, I. Y.: Seasonal circulation and Mauna Loa CO_2 variability, J. Geophys. Res., 111, D13104, doi:10.1029/2005JD006535, 2006.

Masarie, K. A. and Tans, P. P.: Extension and integration of atmospheric carbon dioxide data into a globally consistent measurement record, J. Geophys. Res., 100, 11593–11610, 1995.

Matsueda, H., Machida, T., Sawa, Y., Nakagawa, Y., Hirotani, K., Ikeda, H., Kondo, N., and Goto, K.: Evaluation of atmospheric CO_2 measurements from new flask air sampling of JAL airliner observations, Meteorol. Geophys., 59, 1–17, doi:10.2467/mripapers.2459.2461, 2008.

Matsueda, H. H., Inoue, Y., and Ishii, M.: Aircraft observation of carbon dioxide at 8–13 km altitude over the western Pacific from 1993 to 1999, Tellus, 1–21, 2002.

Miller, J. B., Tans, P. P., White, J. W. C., Conway, T. J., and Vaughn, B. W.: The atmospheric signal of terrestrial carbon isotopic discrimination and its implication for partitioning carbon fluxes, Tellus B, 55, 197–206, 2003.

Miyazaki, K., Patra, P. K., Takigawa, M., Iwasaki, T., and Nakazawa, T.: Global-scale transport of carbon dioxide in the troposphere, J. Geophys. Res., 113, D15301, doi:10.1029/2007JD009557, 2008.

Miyazaki, K., Machida, T., Patra, P. K., Iwasaki, T., Sawa, Y., Matsueda, H., and Nakazawa, T.: Formation mechanisms of latitudinal CO_2 gradients in the upper troposphere over the subtropics and tropics, J. Geophys. Res., 114, D03306, doi:10.1029/2008JD010545, 2009.

Nevison, C. D., Kinnison, D. E., and Weiss, R. F.: Stratospheric influences on the tropospheric seasonal cycles of nitrous oxide and chlorofluorocarbons, Geophys. Res. Lett., 31, L20103, doi:10.1029/2004GL020398, 2004.

Nevison, C. D., Mahowald, N. M., Weiss, R. F., and Prinn, R. G.: Interannual and seasonal variability in atmospheric N_2O, Global Biogeochem. Cy., 21, GB3017, doi:10.1029/2006GB002755, 2007.

Pan, L. L., Hintsa, E. J., Stone, E. M., Weinstock, E. M., and Randel, W. J.: The seasonal cycle of water vapor and saturation vapor mixing ratio in the extratropical lowermost stratosphere, Journal of Geophysical Research, 105, 26519–26530, 2000.

Pan, L. L., Randel, W. J., Gary, B. L., Mahoney, M. J., and Hintsa, E. J.: Definitions and sharpness of the extratropical tropopause: A trace gas perspective, J. Geophys. Res.-Atmos., 109, D23103, doi:10.1029/2004JD004982, 2004.

Pan, L. L., Bowman, K. P., Shapiro, M., Randel, W. J., Gao, R. S., Campos, T., Davis, C., Schauffler, S., Ridley, B. A., Wei, J. C., and Barnet, C.: Chemical behavior of the tropopause observed during the Stratosphere-Troposphere Analyses of Regional Transport experiment, J. Geophys. Res., 112, D18110,, doi:10.1029/2007jd008645, 2007.

Pan, L. L., Randel, W. J., Gille, J. C., Hall, W. D., Nardi, B., Massie, S., Yudin, V., Khosravi, R., Konopka, P., and Tarasick, D.: Tropospheric intrusions associated with the secondary tropopause, J. Geophys. Res., 114, D10302, doi:10.1029/2008jd011374, 2009.

Pataki, D. E., Ehleringer, J. R., Flanagan, L. B., Yakir, D., Bowling, D. R., Stil, C. J., Buchmann, N., Kaplan, J. O., and Berry, J. A.: The application and interpretation of Keeling plots in terrestrial carbon cycle research, Global Biogeochem. Cy., 17, 1022,

Analyses of CO_2 isotope data for tropical troposphere and UT/LMS

S. S. Assonov et al.

doi:1010.1029/2001GB001850, 2003.

Patra, P. K., and Maksyutov, S.: Incremental approach to the optimal network design for CO_2 surface source inversion, Geophys. Res. Lett., 29(10), 1459, doi:10.1029/2001GL013943, 2002.

Patra, P. K., Maksyutov, S., and Group Authors: Transcom 3 Modelers: Sensitivity of Optimal Extension of CO_2 Observation Networks to Model Transport, Tellus, 55B, 498–511, 2003.

Quay, P., Sonnerup, R., Westby, T., Stutsman, J., and McNichol, A.: Changes in the 13C/12C of dissolved inorganic carbon in the ocean as a tracer of anthropogenic CO2 uptake, Global Biogeochem. Cy., 17(1), 1004 doi:10.1029/2001GB001817, 2003.

Rayner, P. J., Law, R. M., Allison, C. E., Francey, R. J., Trudinger, C. M., and Pickett-Heaps, C.: Interannual variability of the global carbon cycle (1992-2005) inferred by inversion of atmospheric CO_2 and $^{13}CO_2$ measurements, Global Biogeochem. Cy., 22, GB3008, doi:10.1029/2007gb003068, 2008.

Rhee, T. S., Brenninkmeijer, C. A. M., Mühle, J., van Velthoven, P. F. J., Hermann, M., Zahn, A., Oram, D. E., Scharffe, D. H., Koeppel, C., Fischer, H., and Lelieveld, J.: A case study of rapid mixing across the extratropical tropopause based on Civil Aircraft for the Regular Investigation of the Atmosphere Based on an Instrumented Container (CARIBIC) observations, J. Geophys. Res. - Atmos., 110, D22301, doi:22310.21029/22005JD005890, 2005.

Schuck, T. J., Brenninkmeijer, C. A. M., Slemr, F., Xueref-Remy, I., and Zahn, A.: Greenhouse gas analysis of air samples collected onboard the CARIBIC passenger aircraft, Atmos. Meas. Tech., 2, 449–464, 2009, http://www.atmos-meas-tech.net/2/449/2009/.

Schuck, T. J., Brenninkmeijer, C. A. M., Baker, A. K., Slemr, F., Velthoven, P. F. J. v., and Zahn, A.: Greenhouse Gas Relationships in the Indian Summer Monsoon Plume Measured by the CARIBIC 2 Passenger Aircraft, to be submitted, Atmos. Chem. Phys. Discuss., 10, 2031–2087, 2010, http://www.atmos-chem-phys-discuss.net/10/2031/2010/.

Shia, R.-L., Liang, M.-C., Miller, C. E., and Yung, Y. L.: CO_2 in the upper troposphere: Influence of stratosphere-troposphere exchange, Geophys. Res. Lett., 33, L14814, doi:10.1029/2006gl026141, 2006.

Still, C. J., Riley, W. J., Biraud, S. C., Noone, D. C., Buenning, N. H., Randerson, J. T., Torn, M. S., Welker, J., White, J. W. C., Vachon, R., Farquhar, G. D., and Berry, J. A.: Influence of clouds and diffuse radiation on ecosystem-atmosphere CO_2 and $CO^{18}O$ exchanges, J. Geophys. Res., 114, G01018, doi:10.1029/2007JG000675, 2009.

Stohl, A., Bonasoni, P., Cristofanelli, P., Collins, W., Feichter, J., Frank, A., Forster, C., Gera-

Title Page	
Abstract	Introduction
Conclusions	References
Tables	Figures
◄◄	►►
◄	►
Back	Close
Full Screen / Esc	

Printer-friendly Version

Interactive Discussion

sopoulos, E., Gaggeler, H., James, P., Kentarchos, T., Kromp-Kolb, H., Kruger, B., Land, C., Meloen, J., Papayannis, A., Priller, A., Seibert, P., Sprenger, M., Roelofs, G. J., Scheel, H. E., Schnabel, C., Siegmund, P., Tobler, L., Trickl, T., Wernli, H., Wirth, V., Zanis, P., and Zerefos, C.: Stratosphere-troposphere exchange: A review, and what we have learned from STACCATO, J. Geophys. Res., 108D12, 8516, doi:10.1029/2002jd002490, 2003.

Strahan, S. E., Douglass, A. R., Nielsen, J. E., and Boering, K. A.: The CO_2 seasonal cycle as a tracer of transport, J. Geophys. Res.-Atmos., 103, 13729–13741, 1998.

Turnbull, J. C., Miller, J. B., Lehman, S. J., Tans, P. P., Sparks, R. J., and Southon, J.: Comparison of 14CO2, CO, and SF6 as tracers for recently added fossil fuel CO_2 in the atmosphere and implications for biological CO_2 exchange, Geophys. Res. Lett., 33, L01817, doi:10.1029/2005gl024213, 2006.

13th_WMO/IAEA_Meeting: 13th WMO/IAEA Meeting of Experts on Carbone Dioxide Concentration and Related Tracers Measurement Techniques, Boulder, Colorado, USA, (WMO TD No. 1359), WMO/GAW report No. 161, http://www.wmo.ch/web/arep/gaw/gawreports.html, Expert Group Recommendations, 19–22 September 2005.

Zahn, A., Brenninkmeijer, C. A. M., Asman, W. A. H., Crutzen, P. J., Heinrich, G., Fischer, H., Cuijpers, J. W. M., and van Velthoven, P. F. J.: Budgets of O_3 and CO in the upper troposphere: CARIBIC passenger aircraft results 1997–2001, J. Geophys. Res.-Atmos., 107(D17), 4337, doi:10.1029/2001jd001529, 2002.

Zahn, A., Brenninkmeijer, C. A. M., and van Velthoven, P. F. J.: Passenger aircraft project CARIBIC 1997–2002, Part II: the ventilation of the lowermost stratosphere, Atmos. Chem. Phys. Discuss., 4, 1119–1150, 2004a,
http://www.atmos-chem-phys-discuss.net/4/1119/2004/.

Zahn, A., Brenninkmeijer, C. A. M., and van Velthoven, P. F. J.: Passenger aircraft project CARIBIC 1997–2002, Part I: the extratropical chemical tropopause, Atmos. Chem. Phys. Discuss., 4, 1091–1117, 2004b, http://www.atmos-chem-phys-discuss.net/4/1091/2004/.

Table 1. Typical 1-σ total uncertainty of the CARIBIC-1 and CARIBIC-2 CO$_2$ data.

	CO$_2$, ppm	δ^{13}C(CO$_2$),‰	δ^{18}O(CO$_2$),‰
CARIBIC-1	0.25	0.022	0.063
CARIBIC-2	0.20	0.020	0.030

Table 2. Annual increase rates (linear fits) for the NOAA stations.

Variable	Stations	Data source	Years	Increase rate
CO$_2$	MLO, KUM, MID	NOAA ftp server (GLOBALVIEW-CO$_2$:, 2009)	1999-2007	2.04 ppm/y
δ^{13}C(CO$_2$)	MLO, KUM	NOAA ftp server (GLOBALVIEW-CO2C13)	1999–2007	−0.032‰/y
N$_2$O	MLO, KUM, IZO, AZR (flask samples)	NOAA (Dlugogencky, 2009)	1998–2008	0.76 ppb/y
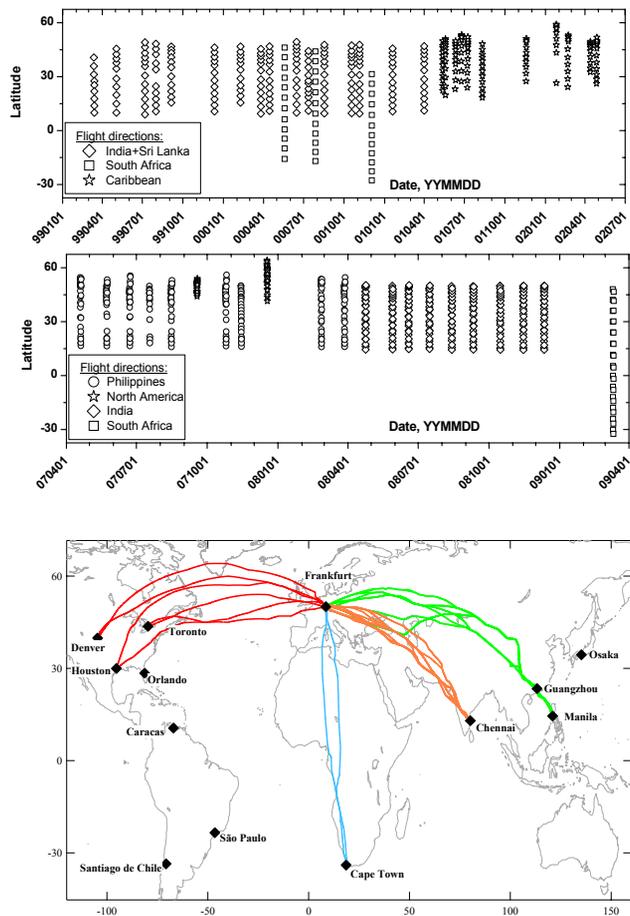
Fig. 1. CARIBIC-1 (upper panel) and CARIBIC-2 (middle panel) sample distribution used for CO_2 isotope analyses. Lower panel, CARIBIC-2 flight routes.
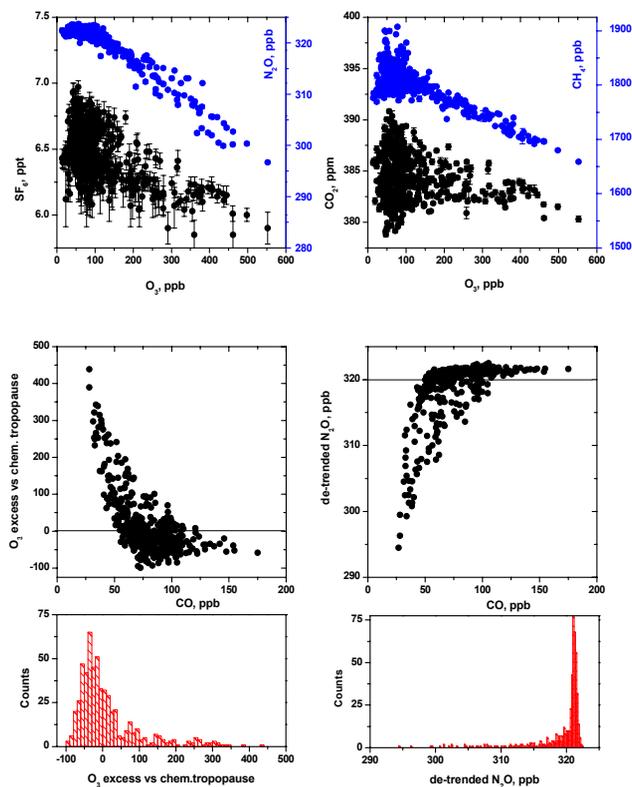
Fig. 2. Upper panel: GHG data (N_2O, SF_6, CH_4 and CO_2) for CARIBIC-2, flights of April 2007 to March 2009 (period covered by CO_2 isotope analyses) plotted against ozone. The data are not de-trended and UT, tropical FT, and LMS samples are all plotted together. Lower panel: Comparison of stratospheric tracers. De-trended N_2O data vs. CO demonstrate a more compact distribution than O_3 vs. CO. To enable a comparison histograms of O_3 and N_2O are given.
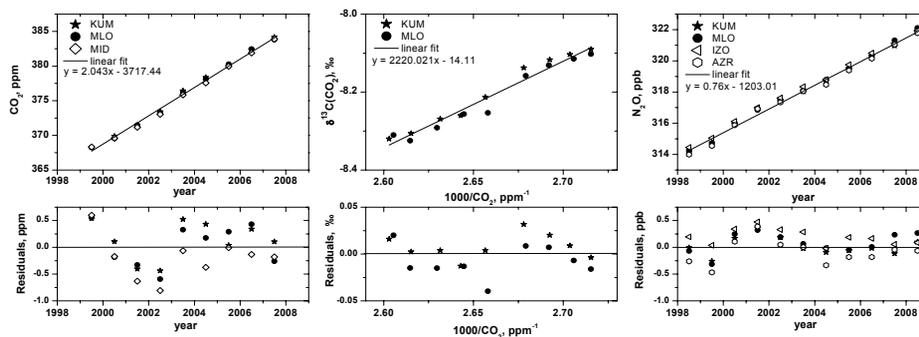
Fig. 3. Linear fits through annual means of CO_2, $\delta^{13}C(CO_2)$ and N_2O for selected/background NOAA stations, see Table 1. Residuals are shown in lowermost panels. To demonstrate the consistency between $\delta^{13}C(CO_2)$ increase rate with the CO_2 increase, $\delta^{13}C(CO_2)$ is plotted vs. $1/CO_2$, see text.

ACPD

10, 5999–6057, 2010

Analyses of CO$_2$ isotope data for tropical troposphere and UT/LMS

S. S. Assonov et al.

Title Page

Abstract | Introduction

Conclusions | References

Tables | Figures

◄ | ►►

◄ | ►

Back | Close

Full Screen / Esc

Printer-friendly Version

Interactive Discussion
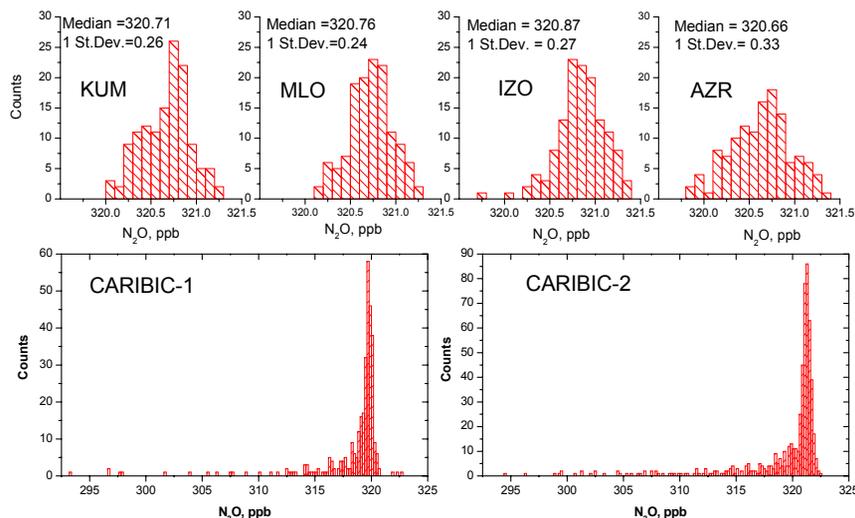
Fig. 4. Upper panel: Distribution of de-trended, monthly mean N$_2$O data for NOAA stations in the NH tropics, 1998 to 2008. The distributions are slightly skewed presumably due to deviations of N$_2$O increase in 1999 and 2001 from the linear trend (see Fig. 3). Lower panel: Distribution of de-trended N$_2$O data for CARIBIC-1 and CARIBIC-2. Majority of samples represent FT and UT air masses and have N$_2$O above 320.0 ppb; the tailing to lower N$_2$O values is due to the contribution of LMS air masses.

Title Page

Abstract Introduction

Conclusions References

Tables Figures

◄◄ ►►

◄ ►

Back Close

Full Screen / Esc
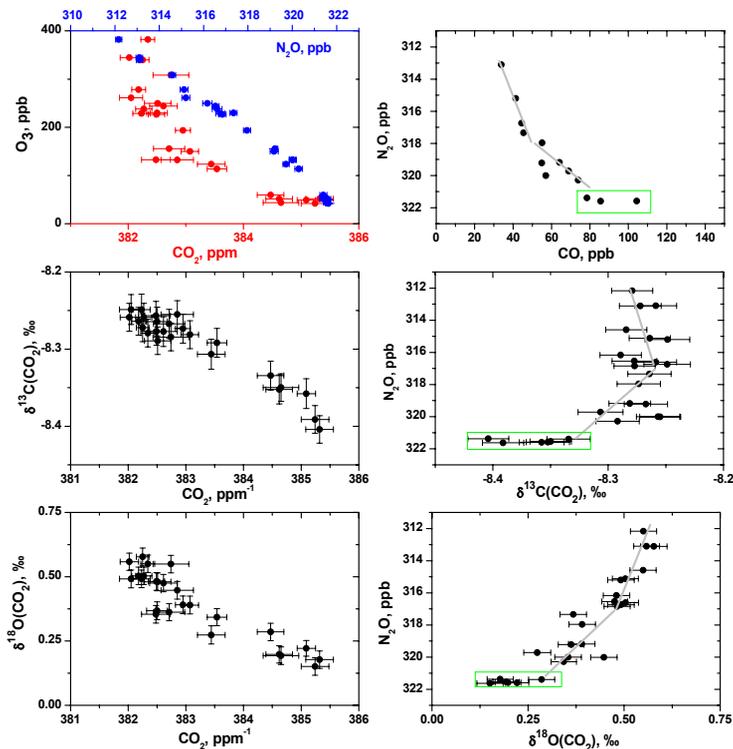
Fig. 5. Example flight Frankfurt-Denver-Frankfurt (17–18 December 2007, latitudes 41 to 63° N) crossing the tropopause and demonstrating anti-correlations between O$_3$, CO and GHG data. The CO$_2$ isotope data vs. N$_2$O demonstrate the same L-shape mixing plot (due to UT/LMS mixing) as typically recorded by O$_3$ and CO. The CO$_2$ isotope data plotted vs. CO$_2$ give linear mixing trends. The correlation between isotope data and stratospheric tracers (N$_2$O and O$_3$) is observed for majority of flights that crossed the UT/LMS mixing. Data in the green boxes show UT samples.
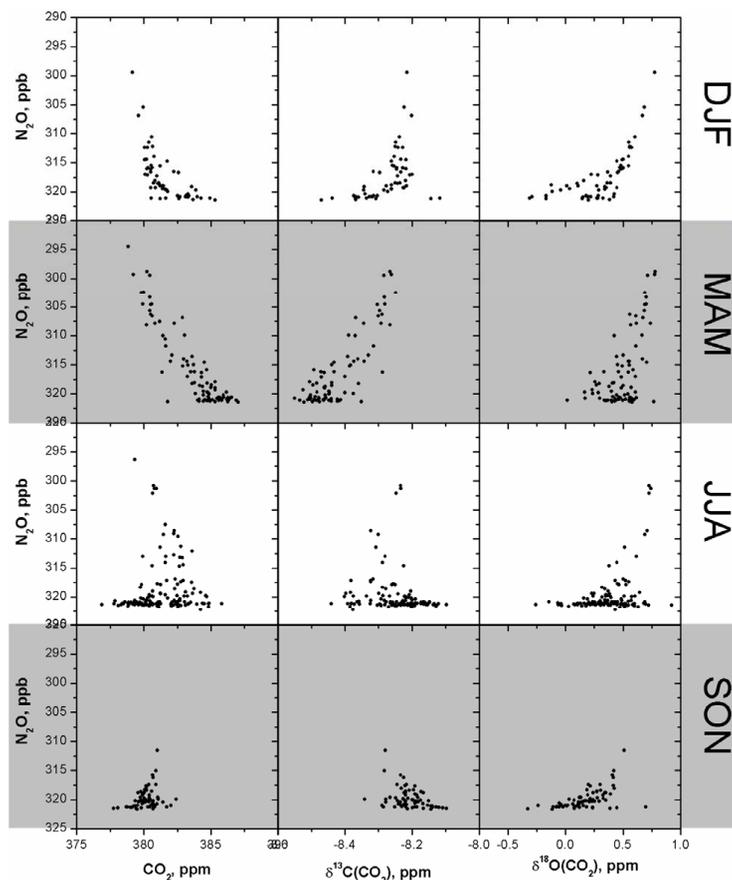
Fig. 6. CARIBIC-2 CO_2 isotope data separated in 4 different seasons and plotted versus the stratospheric tracer N_2O. Plotted are latitudes above 35° N where UT/LMS mixing takes place. Seasonal variability of UT/LMS trends observed is governed mostly by variability in the UT air.
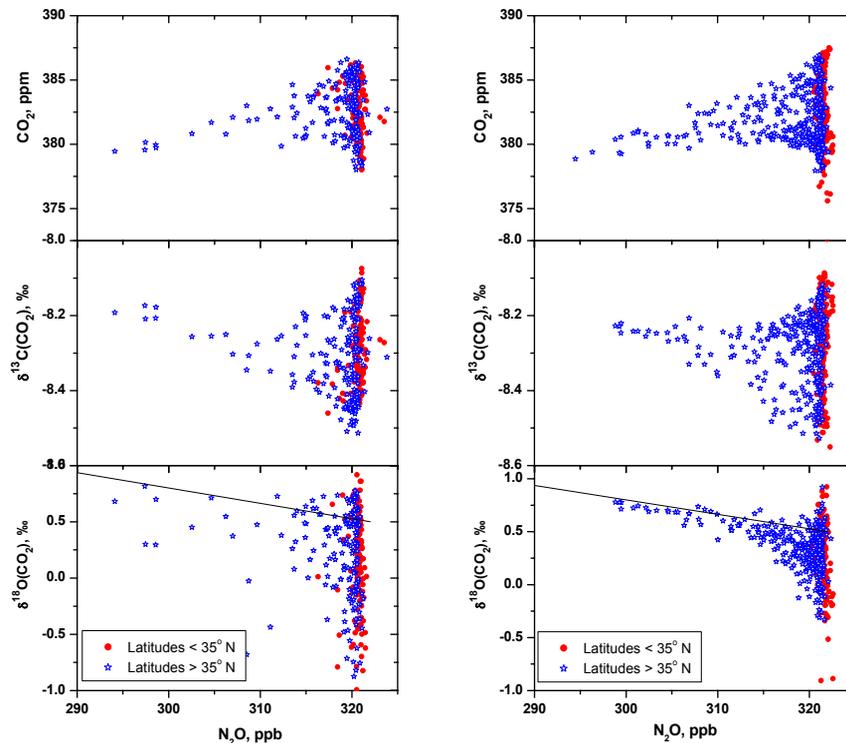
Fig. 7. The UT/LMS mixing trends for CARIBIC-1 (left) and CARIBIC-2 (right). For CARIBIC-2 the trends are visible both in CO_2, $\delta^{13}C(CO_2)$ and in $\delta^{18}O(CO_2)$. The CARIBIC-1 $\delta^{18}O(CO_2)$ data are qualitative only. UT/LMS mixing trends form triangle-shaped areas; this mixing affects latitudes above 35 °N only. The trend line for $\delta^{18}O(CO_2)$ is evaluated based on the data for stratospheric CO_2, see text.

Title Page

Abstract | Introduction

Conclusions | References

Tables | Figures

◄ | ►

Back | Close

Full Screen / Esc

Printer-friendly Version

Interactive Discussion
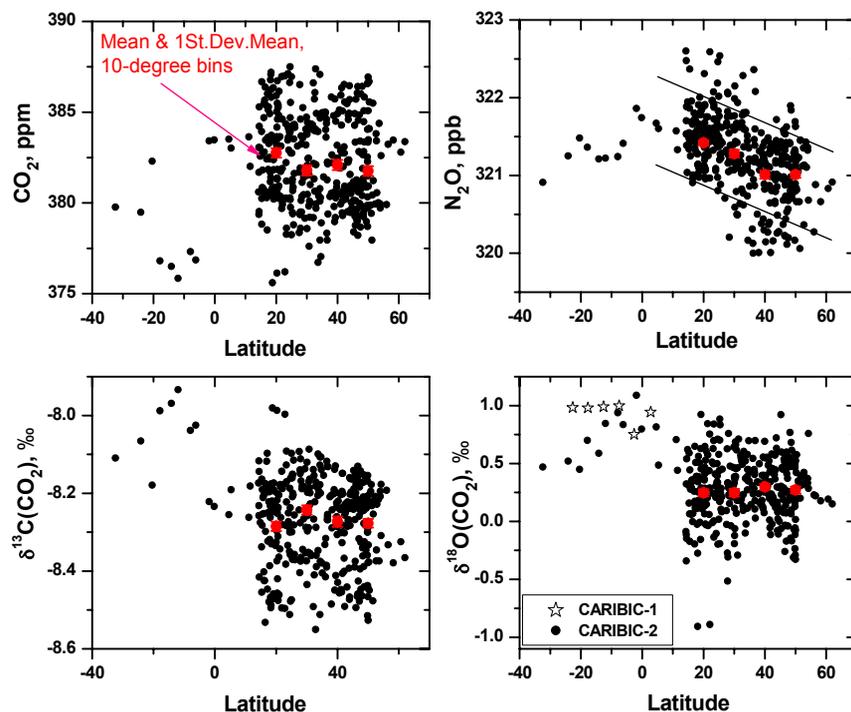
Fig. 8. Latitudinal distribution of CO_2, N_2O and isotope data for CARIBIC-2, flights of April 2007 to March 2009 (de-trended data). Only UT and FT samples of CARIBIC-2 (separated by $N_2O>320.0$ ppb) and $\delta^{18}O(CO_2)$ values of CARIBIC-1 in the SH are shown. Shown in red are mean values in 10-degree bands, the error bars (close to symbol size) correspond to 1 St.Error of the Mean.
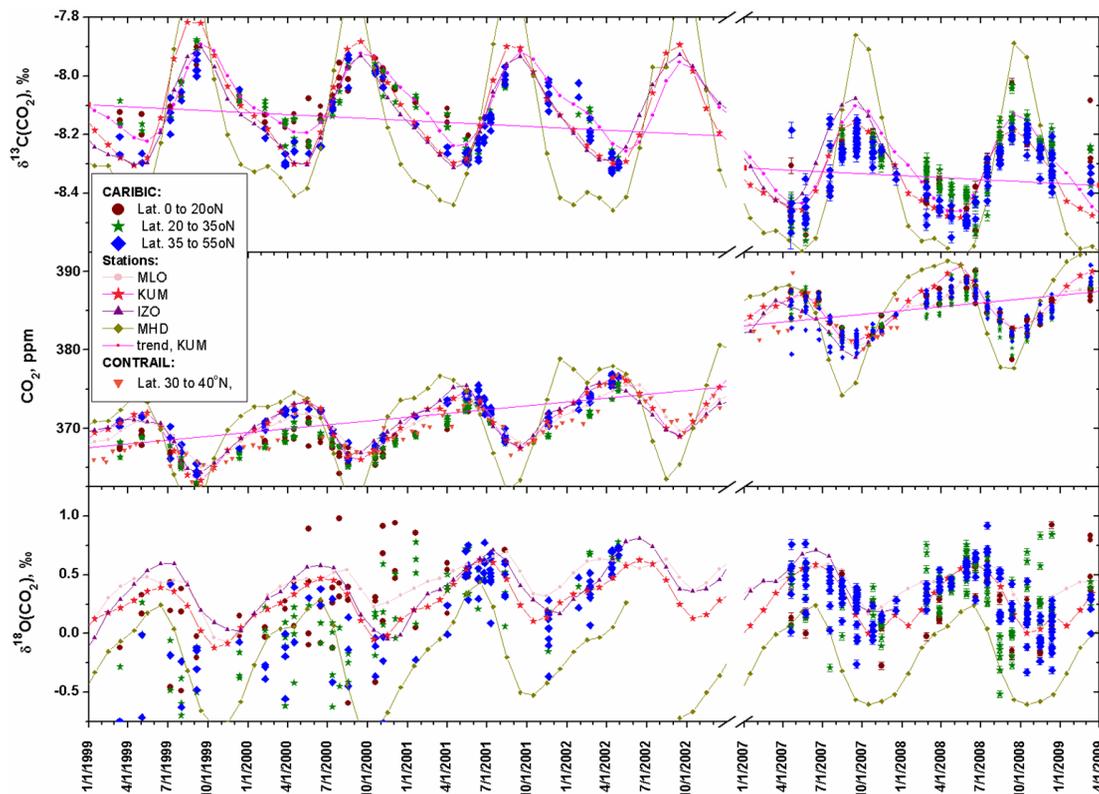
Fig. 9. CO_2, $\delta^{13}C(CO_2)$ and $\delta^{18}O(CO_2)$ data of CARIBIC-1 and CARIBIC-2 as time series together with data for the stations (MLO, KUM, IZO and MHD, GLOBALVIEW-CO2, 2009; GLOBALVIEW-CO2C13) and CONTRAIL (latitudes 30 to 40° N, CONTRAIL, 2009). The linear trend lines are given for KUM. (For allowing a comparison, station isotope data are extrapolated from 01/01/2008 to 04/01/2009 as based on the data for 2008 and the annual increase rates, Table 2).

Title Page

Abstract | Introduction

Conclusions | References

Tables | Figures

|◄ | ►|

◄ | ►

Back | Close

Full Screen / Esc

Printer-friendly Version

Interactive Discussion
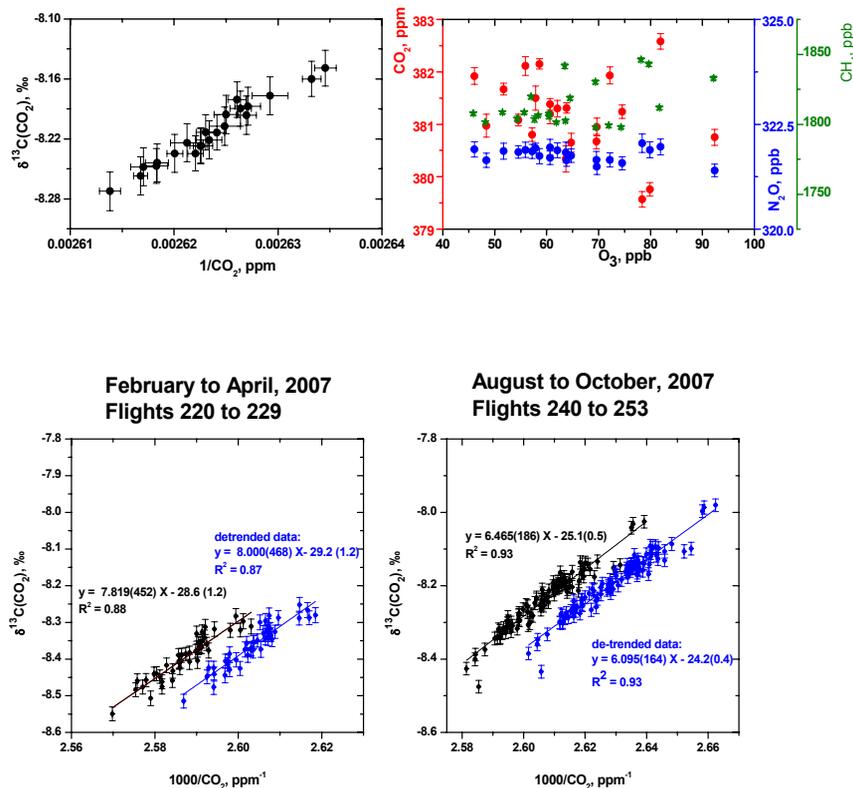
Fig. 10. Upper panel: For a single flight (Frankfurt-Toronto-Frankfurt, September 2007, latitudes 44 to 54° N) an excellent correlation with an extremely narrow range of $\delta^{13}C(CO_2)$ values was observed for UT air masses. The correlation exists despite of different air masses, as demonstrated by the variability in methane. Right, GHG data for the same flight plotted vs. O$_3$ demonstrate stable levels of N$_2$O and variable methane. Lower panel: CARIBIC-2 data, Keeling plots of $\delta^{13}C(CO_2)$ for different seasons. De-trended data (in blue) demonstrate a bit different slopes.
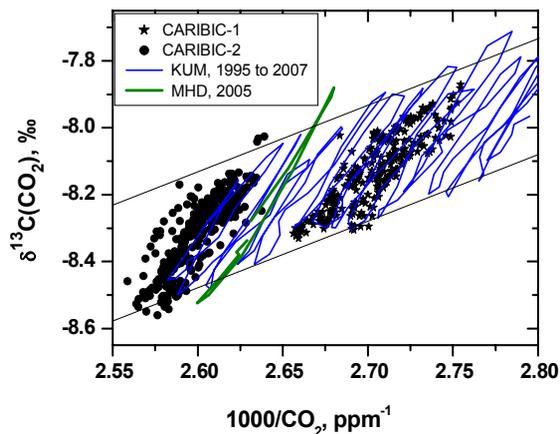
Fig. 11. Keeling plot for CARIBIC-1 and CARIBIC-2 (data not de-trended) including KUM (years 1993 to 2007) and MHD (year 2005). The two enveloping lines correspond to the slope of the KUM inter-annual trend, and give upper and lower limits of the variability. CARIBIC data agree well with the range demonstrated by the tropical station. Some CARIBIC-2 data points above the indicated range are probably affected by SH air (higher $\delta^{13}C(CO_2)$) and/or by photosynthesis uptake (also higher $\delta^{13}C(CO_2)$). The shift between CARIBIC-1 and CARIBIC-2 corresponds to the global CO$_2$ increase.
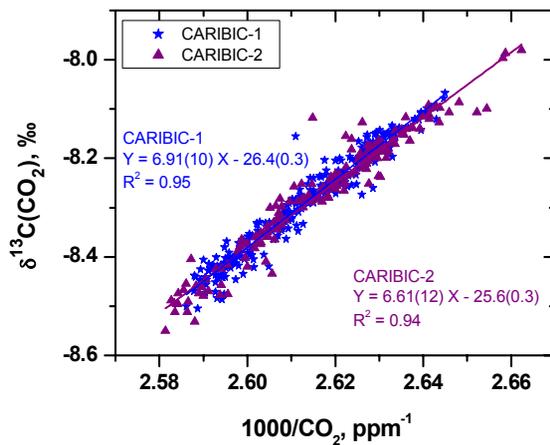
Fig. 12. Keeling plots for $\delta^{13}C(CO_2)$ for de-trended CARIBIC-1 and CARIBIC-2 data showing close agreement (all seasons, data de-trended to 1/01/2007).
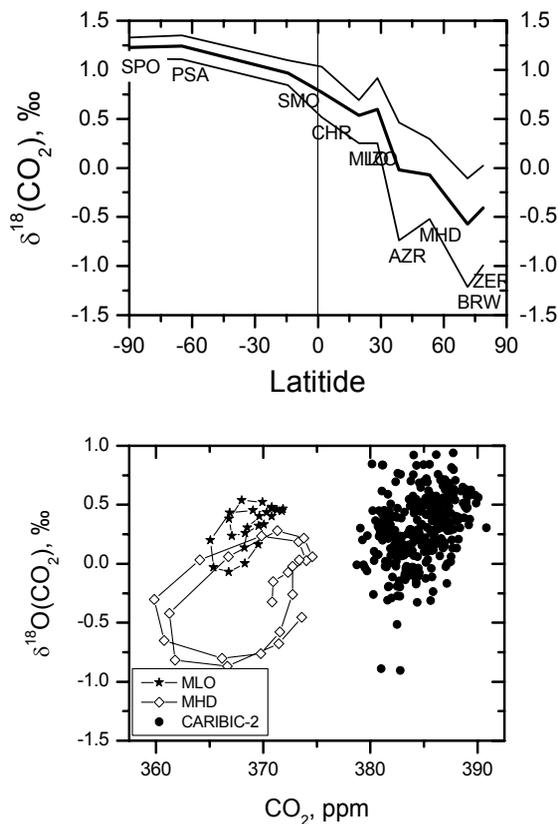
Fig. 13. Upper panel: Global latitudinal gradient of the $\delta^{18}O(CO_2)$ seasonal cycle, data for NOAA stations (GLOBALVIEW-CO2C13). Mean values and the amplitudes, averaged for years 2003 to 2005. Lower panel: The $\delta^{18}O(CO_2)$ seasonal cycle at Mauna Low and Mace Head, years 1999–2000. The cycle direction is anti-clock wise. CARIBIC-2 data: UT and FT air, latitudes > 14° N.
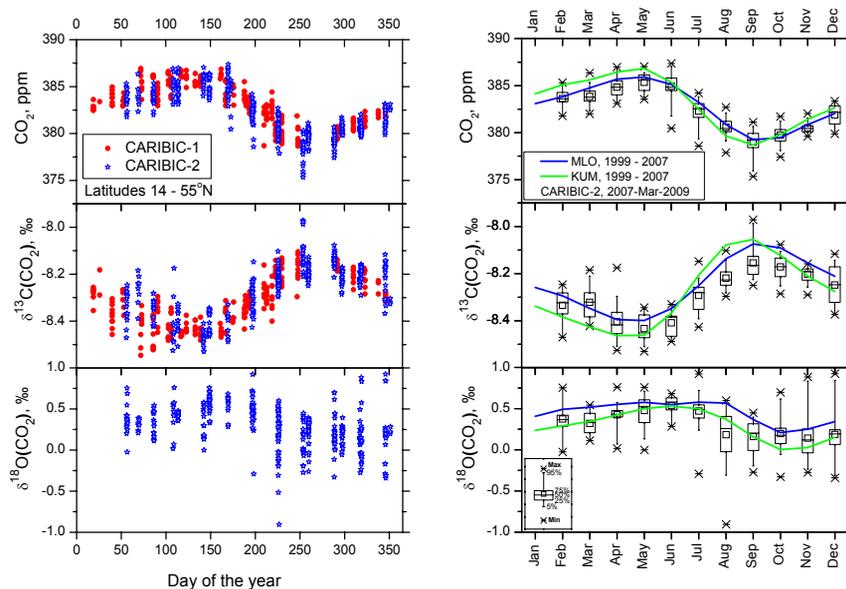
Fig. 14. Left: Seasonality for FT and UT air masses detected by CO_2 isotopes; all flights. Data de-trended to 1/1/2007. Right: FT and UT CARIBIC-2 data (box-plot) and the 1999 to 2007 averaged monthly mean data for KUM and MLO. Plumes evidenced by very high water and high CO are filtered out ($H_2O>2000$ ppm and CO>125 ppb).

Title Page

Abstract | Introduction

Conclusions | References

Tables | Figures

◄◄ | ►►

◄ | ►

Back | Close

Full Screen / Esc

Printer-friendly Version

Interactive Discussion